VERTEBRATE ZOOLOGY

70 (2): 241–262
2020

SENCKENBERG

A revised phylogeny of nuthatches (Aves, Passeriformes, *Sitta*) reveals insight in intra- and interspecific diversification patterns in the Palearctic

Martin Päckert[1,2,*], Marcella Bader-Blukott[1], Berit Künzelmann[1], Yue-Hua Sun[3], Yu-Cheng Hsu[4], Christian Kehlmaier[1], Frederik Albrecht[1], Juan Carlos Illera[5] & Jochen Martens[6]

[1] Senckenberg Naturhistorische Sammlungen, Museum für Tierkunde, Königsbrücker Landstr. 159, 01109 Dresden, Germany — [2] Senckenberg Biodiversity and Climate Research Centre, Senckenberganlage 25, 60325 Frankfurt am Main, Germany — [3] Key Laboratory of Animal Ecology and Conservation, Institute of Zoology, Chinese Academy of Sciences, Beijing 100101, People's Republic of China — [4] Department of National Resources and Environmental Studies, National Dong Hwa University, Shou-Feng, 974 Hualien, Taiwan — [5] Research Unit of Biodiversity (UO-CSIC-PA), Oviedo University, Campus of Mieres, Research Building, 5th Floor. C/ Gonzalo Gutiérrez Quirós, s/n, 33600 Mieres, Asturias, Spain — [6] Institut für Organismische und Molekulare Evolutionsbiologie (iomE), Johannes Gutenberg-Universität Mainz, 55099 Mainz, Germany — * Corresponding author, e-mail: martin.paeckert@senckenberg.de

Submitted May 14, 2019.
Accepted May 10, 2020.
Published online at www.senckenberg.de/vertebrate-zoology on May 29, 2020.
Published in print Q2/2020.

Editor in charge: Uwe Fritz

Abstract

Nuthatches of the Holarctic and partly Indo-Malayan genus *Sitta* have been subject to a number of phylogenetic analyses; however, the most complete phylogenetic hypothesis to date missed several Asian species-level taxa, was based on a limited sampling, and included only one sample per species. Other recent studies were mainly focused on phylogeographic patterns of single Asian species but failed to unambiguously resolve their phylogenetic relationships. In this study, we provide a time-calibrated multi-locus phylogeny of nuthatches (*Sitta*) including 27 out of 28 currently recognized species. To account for intraspecific variation we included a number of subspecific taxa in our sampling, e.g. for the phenotypically diverse Eurasian nuthatch, *S. europaea*. Within the latter species (our clade X) three phenotypically distinct phylogroups started diversifying from the early Pleistocene on: (i) brown-bellied forms of the *sinensis* group from China and Taiwan with smallest body size dimensions, (ii) white-bellied forms of the Central and Eastern Palearctic *europaea* group with average body size dimensions, and (iii) brown-bellied forms of the Western Palearctic and Caucasian *caesia* group with largest body size dimensions. The three phylogroups are connected by chains of phenotypically intermediate populations in Eastern Europe (e.g. ssp. *homeyeri*) and in Far East Russia and north-eastern China (ssp. *amurensis*).

The Eurasian nuthatch was sister to a monophyletic clade IX comprising five Sino-Himalayan species: *S. nagaensis*, *S. cashmirensis*, *S. castanea*, *S. neglecta,* and *S. cinnamoventris*. In the Sino-Himalayas, ecological segregation along the elevational gradient was established from the mid-Miocene onset of nuthatch diversification until the recent ecological segregation among chestnut-bellied forms of the *S. castanea* complex during the Pleistocene.

Key words

Biometry, elevational parapatry, phylogeography, phylogroups, Sino-Himalayas, *Sitta arctica*, *Sitta europaea*.

Introduction

Nuthatches (*Sitta*) are the most speciose genus of the passerine family Sittidae that according to current systematics includes two further genera of subfamily rank: the monotypic wallcreeper (*Tichodroma muraria*; Tichodrominae) and spotted creepers (*Salpornis*, Salpornithinae; Dickinson & Christidis, 2014; del Hoyo & Collar,

2016; Clements *et al*. 2017). However, this classification was recently challenged by a molecular phylogeny that placed *Salpornis* as sister of treecreepers (*Certhia*) and the wallcreeper, *Tichodroma*, as sister of the nuthatches (Zhao *et al.*, 2016). These phylogenetic relationships are in good accordance with traditional classifications of Sittidae and Certhiidae (e.g. Harrap & Quinn, 1996). Based on phylogenetic hypotheses Cracraft *et al*. (2004) grouped Sittidae and Certhiidae (including *Tichodroma* and *Salpornis*) together with gnatcatchers (Polioptidae) and wrens (Troglodytidae) in the superfamily Certhioidea. However, within Certhioidea the phylogenetic relationships among these four families are unresolved so far (Zhao *et al*. 2016).

The species of nuthatches of genus *Sitta* are forest-dwelling passerines, except the rock nuthatches (*S. neumayer* and *S. tephronota*). Their diversity hotspot lies in the Sino-Himalayas and the adjoining Indo-Burmese mountain ranges in the Southwest where a number of narrow-range endemics occur. Current taxonomic authorities recognize 25 species (Dickinson & Christidis, 2014) to 29 species (del Hoyo & Collar, 2016). In this study we rely on the species-level classification by Gill *et al.* (2020) who distinguish 28 species.

A first single-locus phylogeny had a focus on the relationships of Nearctic and some Palearctic species (Pasquet, 1998). A recent multi-locus phylogeny comprised 21 out of 28 species-level taxa and revealed a complex radiation from an Asian center of origin (Pasquet *et al.*, 2014). From this near-complete phylogeny the following species were missing: (i) from the Sino-Himalayas *S. castanea*, *S. cinnamoventris*, *S. neglecta,* and *S. leucopsis*; (ii) one endemic of the Indo-Burmese Biodiversity Hotspot, *S. victoriae*; (iii) *S. solangiae* from Hainan and adjacent Southeast Asia; and (iv) *S. arctica* from northeast Siberia. There has been a long debate on the taxonomic status and the systematic affiliation of the latter enigmatic Siberian nuthatch or taiga nuthatch from far northeastern Russia (Fig. 1A; Red'kin & Konovalova, 2006; Harrap, 2008). Traditionally, the form *arctica* has been treated conspecific with *S. europaea* (Vaurie, 1959; Harrap & Quinn, 1996; Harrap, 2008) and was included as one of its subspecies by some authors until recently (Clements *et al*., 2017). However, because of strong evidence of its genetic distinctiveness against *S. europaea* (Zink *et al*., 2006; Hung *et al*., 2012), *S. arctica* has been recently upgraded to species level by several taxonomic authorities (Dickinson & Christidis, 2014; del Hoyo & Collar, 2016; Gill *et al*., 2020). Recent findings have suggested that *S. arctica* is only distantly related to a monophyletic group of *S. europaea*, *S. cashmirensis,* and *S. nagaensis*; however, its phylogenetic relationships to these species and to *S. himalayensis* were not well resolved (Chen *et al*., 2019).

A further limitation of the nuthatch phylogeny by Pasquet *et al.* (2014) was that only a single sample per species was analyzed, and thus intraspecific differentiation was not taken into account. However, phylogeographic structure is commonly found in widespread polytypic bird species and therefore warrants detailed consideration (Illera *et al*., 2008; Albrecht *et al*., 2020). In the Nearctic, phylogeographic structure was documented in the white-breasted nuthatch, *S. carolinensis* (Spellman & Klicka, 2007; Walstrom *et al.*, 2011) but was lacking for example in the widespread pygmy nuthatch, *S. pygmaea* (Spellman & Klicka, 2006). Among-island diversification was found in the sulphur-billed nuthatch, *S. oenochlamys*, from the Philippines (Campbell *et al*., 2016). Furthermore, in the Palearctic substantial intraspecific differentiation was found in the Eurasian nuthatch, *S. europaea*, with three major genetic lineages to be distinguished in (i) the Western Palearctic, (ii) the Eastern Palearctic, and (iii) in the Caucasus (Zink *et al.*, 2006; Hung *et al.*, 2012). Recent studies identified two further Caspian mitochondrial lineages of *S. europaea* from Iran (Nazarizadeh *et al*., 2016) and another distinct Chinese lineage including the subspecies *S. e. sinensis* and *S. e. formosana* (Chen *et al.*, 2019). Still, intraspecific molecular-genetic diversification of the Eurasian nuthatch might be underestimated because of its substantial trans-Palearctic morphological variation among 21 currently accepted subspecies (Harrap, 2008; Gill *et al*., 2020).

Close relationships of *S. europaea* and the Himalayan species complex of *S. castanea*, *S. neglecta*, *S. cinnamoventris*, *S. cashmirensis,* and *S. nagaensis* have long been considered. In the 20th century many of these taxa were treated on a subspecific level: Vaurie (1950, 1959) included all of them in *S. europaea*, whereas others included *cinnamoventris* and *neglecta* in *S. castanea* but ranked *S. cashmirensis* and *S. nagaensis* as full species (Harrap & Quinn, 1996; Dickinson & Christidis, 2014). Particularly the species status of the chestnut-vented nuthatch, *S. nagaensis*, remained subject of a controversial discussion until recently (Dickinson, 2006). Previous phylogenies confirmed a monophyletic clade of *S. europaea*, *S. nagaensis,* and *S. cashmirensis*, but with conflicting topologies inferred from different tree reconstructions (Pasquet *et al.*, 2014; Chen *et al*., 2019). Apart from phenotypical diagnosability, these nuthatch species occupy various ecological forest niches along the Sino-Himalayan elevational gradient (Fig. 1B). At higher elevations the Kashmir nuthatch, *S. cashmirensis*, is a near-endemic of the Western Himalayan Sub-alpine Conifer Forests (WWF Ecoregion IM0502; region 29 in Wikramanayake *et al*., 2002). In the Central Himalayas the chestnut-bellied nuthatch, *S. cinnamoventris* settles subtropical open deciduous forests at the Himalayan foothills up to 1560 m (Inskipp & Inskipp, 1991; Martens & Eck, 1995; Harrap, 2008). In the East its breeding range extends across the Indo-Burmese mountain systems to northern Vietnam, where it overlaps with the ranges of two of its closest relatives: The Burmese nuthatch, *Sitta neglecta*, settles dry dipterocarp and pine forests of the Burmese mountain systems with an upper range limit up to 1000 m in Myanmar, whereas the chestnut-vented nuthatch, *S. nagaensis*, occupies montane evergreen and pine forests at a higher elevational belt up to 2800 m at Mount Victoria (Mynamar) and up to 4570 m in Yunnan (Harrap &

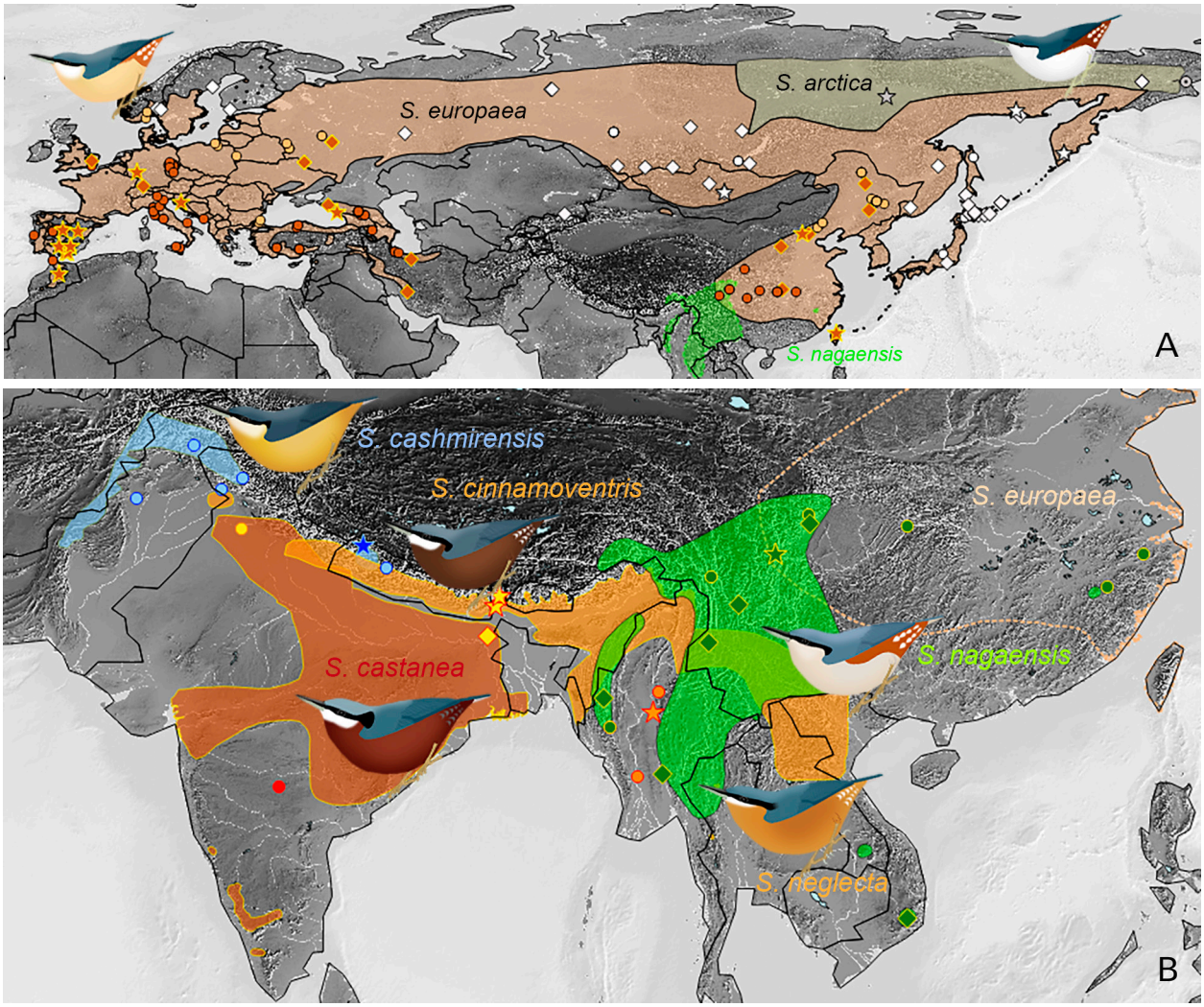

Fig. 1. Origin of study material of **A**: the Eurasian nuthatch (*Sitta europaea*: one white-bellied and two brown-bellied subspecies groups indicated by symbol colors; intermediate phenotypes of ssp. *homeyeri* in the West and ssp. *amurensis* in the East indicated by pale ocher symbols) and the Siberian nuthatch (*S. arctica*); **B**: their Sino-Himalayan counterparts of the *S. castanea* species compex; dots: specimens examined; diamonds: sequence data from GenBank; stars: own samples for sequence analysis; distribution ranges indicated by shape files downloaded from BirdLife International and NatureServe (2015); nuthatch graphics by Totodu & Shyamal (2008).

Quinn, 1996; Harrap, 2008). A recent phylogeographic study suggested that this species comprises six highly diverged mitochondrial lineages that correspond to only four subspecific taxa (Zhao *et al*., 2019). Finally, the Indian nuthatch, *S. castanea*, is the only member of the group that is not restricted to montane habitats. It is distributed across the Indian Subcontinent where it settles lowland forests as well as anthropogenic habitats like gardens and parks and subtropical moist montane forests of the Western Ghats and Eastern Ghats and of the Himalayan forelands in southwestern Nepal. The phylogenetic relationships of these five species are barely understood and an approximate time estimate for the origin of their radiation is missing, to date.

In this study we aim at completing the phylogeny of *Sitta* with a particular focus on: 1) phylogeographic structure within *S. europaea*; 2) phylogenetic relationships of Sino-Himalayan nuthatches of the *S. castanea* group; and 3) phylogenetic relationships of *S. arctica*. In addition, our molecular analyses are flanked by a morphological study including biometric measurements and phenotypic comparison of specimens from bird collections.

Material and Methods

Classification of subspecies-level taxa

Subspecies in ornithology: When criteria for the delimitation of subspecies were first defined in ornithology, a subspecies name referred to a certain phenotypical variant within a range of intraspecific geographical variation (Chapman, 1924; Mayr, 1943). Such variation of phenotypic traits was generally assumed to be clinal across a continuous range and divergent phenotypes should be connected by intermediate phenotypes across broader or narrower zones of intergradation (Mayr, 1943, 1982;

Wilson & Brown, 1953). When newly established bioacoustic and genetic methods during the last decades of the 20th century shaded new light on what do date was assumed intraspecific variation, species rank was consequently assigned to a great number of former subspecies. Nevertheless, the controversial debate on the necessity of a subspecies category and possible thresholds distinguishing species level from subspecies level persisted (Zink, 2004; Philimore & Owens, 2006). While at the beginning of the 21st century molecular taxonomy still struggled with the diverse pitfalls of mtDNA-based phylogenies (e.g. with respect to species-level paraphyly: Funk & Omland, 2003; Kizirian & Donelly, 2004; Pratt, 2010), successive population genetic studies allowed for assessment of gene flow across known zones of intergradations among phenotypically divergent subspecific taxa. As an example from the Western Palearctic, genetically distinct populations of the coal tit, *Periparus ater*, from the European Mediterranean coast and from Scandinavia are connected by clinally intergrading phenotypes and genetically admixed populations from Germany belonged to the phenotypically intermediate subspecies *P. a. abietum* (Pentzold *et al*., 2013; Tritsch *et al*., 2018). Today, integrative taxonomic approaches emphasize that subspecies-level taxa should represent distinct genetic lineages (of both mitochondrial and nuclear genomes), while admixture in regions of secondary overlap and gene flow is generally possible (Kindler & Fritz, 2018). Because lack of reproductive isolation is a key criterion for subspecies-level taxa (Patten *et al*., 2010; Patten, 2015), essentially the subspecies category is a component of the biospecies concept (BSC) (Kindler & Fritz, 2018). Any subspecies classification based on the criteria of the phylogenetic species concept (PSC) has strong limitations by definition. Subspecies-level taxa cannot be fully diagnosable and the debate on possible identification thresholds continues on (i.e. how many percent of individuals from a local population should be identifiable at the subspecies level; Rising, 2007; Martien *et al*., 2017). Reciprocal monophyly is not a good criterion for subspecies delimitation either (see for example Wallin *et al*., 2017) and Patten (2015) even argued that under the PSC a lack of reciprocal monophyly among phenotypically diagnosable taxa should imply subspecies rank.

Subspecies groups of *Sitta europaea*: To complicate things, ornithological taxonomy and systematics often refer to subspecies groups as a further category of intraspecific classification. In the Eurasian nuthatch, *S. europaea*, three major subspecies groups are traditionally recognized according to plumage coloration and body size proportions (Fig. 1A): (i) the buff-breasted western Palearctic *caesia* group, (ii) the white-breasted north-northeastern Palearctic *europaea* group, and (iii) the buff-breasted East Asian *sinensis* group (Voous & van Marle, 1953; Vaurie, 1959; Harrap & Quinn, 1996). Currently, del Hoyo & Collar (2016) distinguish largely the same three subspecific groups under the vernacular names (i) European nuthatch (*caesia* group *sensu* Harrap & Quinn, 1996; including the white-breasted nominate form *S. e. europaea*), (ii) Asian nuthatch (*europaea* group *sensu* Harrap & Quinn, 1996; without *S. e. europaea*), and (iii) Oriental nuthatch (*sinensis* group *sensu* Harrap & Quinn, 1996). Zones of intergradations between the white-bellied subspecies group of the Central and Eastern Palearctic and the adjacent buff-bellied subspecies groups extend from Eastern Europe to western Russia in the West and from Primorye Region in the Russian Far East across the Korean Peninsula to North China in the East (Fig. 1).

In the present study, we follow the classification of delHoyo & Collar (2016) for description of phylogroups in *S. europaea*.

Taxon sampling

We analyzed 68 samples of 27 currently recognized *Sitta* species. The sample material included 11 out of 21 currently recognized subspecies of the widespread Eurasian nuthatch, *Sitta europaea*, namely *albifrons*, *asiatica, amurensis*, *baicalensis*, *caesia*, *caucasica*, *cisalpina*, *formosana*, *hispaniensis*, *sakhalinensis,* and *sinensis* (Table S1). We furthermore included the following nuthatch species that have been missing from the phylogeny by Pasquet *et al*. (2014) into our data set: *S. arctica*, *S. castanea*, *S. cinnamoventris, S. leucopsis, S. neglecta*, and *S. victoriae.* Likewise, the final sequence data set of own samples and GenBank downloads comprised all *Sitta* species recognized by Gill *et al*. (2020) except *S. solangiae* from Southeast Asia of which we could not gather any material (for the total sampling and origin of samples see Table S1). We also included sequences downloaded from GenBank from further subspecies of *S. europaea* (ND2: *S. e. clara*, *S. e. europaea*, *S. e. persica*, *S. e. rubiginosa*; COI: *S. e. hondoensis*, *S. e. takatsukatsai*; Table S1). With those additional taxa our final data set included 17 out of 21 subspecies of the Eurasian nuthatch missing out only *S. e. levantina* from southern Turkey and western Syria, *S. e. bedfordi* from Jeju Island (offshore South Korea), *S. e. roseilla* from southern Kyushu Islands (Japan), and *S. e. seorsa* from the Chinese Altai Mountains. As further outgroup taxa of Certhioidea we included sequence data from GenBank for two wren species (*Troglodytes troglodytes*, *T. aedon*), two gnatcatcher species (*Polioptila caerulea*, *P. dumicola*), the wallcreeper (*Tichodroma muraria*), and the African spotted creeper, *Salpornis salvadori*.

Laboratory procedures

DNA was extracted using Qiagen DNEasy Blood & Tissue Kits (Qiagen, Inc.) according to the manufacturer's instructions. Our material included toe-pad material of three so far unstudied species (*S. castanea*, *S. cinnamoventris*, *S. victoriae*) missing from the phylogeny by Pasquet *et al*. (2014). Toe pads were taken from six specimens from the Museum of Zoology (MTD), Senck-

Table 1. Primer pairs used for PCR and sequencing; *= primer used for sequencing only.

marker		primers	primer sequence (5‘-3‘)	reference	PCR settings
Cytb	Forward	OL-14851	CCTACCTAGGATCATTCGCCCT	Weir & Schluter (2007)	94°C – 10 min
	Reverse	OH-16065	AGTCTTCAATCTTTGGCTTACAAGAC		92°C – 1 min 53°C – 1min 72°C – 2 min 35 cycles
					72°C – 10 min
ND2	Forward	NDL 5216	GGCCCATACCCCGRAAATG	Sorenson *et al.* (1999)	94°C – 10 min
	Reverse	NDH 6313	ACTCTTRTTTAAGGCTTTGAAGGC		92°C – 1 min 53°C – 1min 72°C – 2 min 35 cycles
					72°C – 10 min
COI	Forward	Bird F1	TTCTCCAACCACAAAGACATTGGCAC	Hebert *et al*. (2004); Dove *et al.* (2008)	94°C – 5 min
	Reverse	Bird R1	ACGTGGGAGATAATTCCAAATCCTG		92°C – 1 min 50°C – 1:30min 72°C – 1:30 min 5 cycles 92°C – 1 min 51°C – 1:30min 72°C – 1:30 min 30 cycles
	Reverse	COIR*	ACTTCTGGGTGGCCAAAGAATCAGAA		72°C - 5 min
myo	Forward	myo2	GCCACCAAGCACAAGATCCC	Johansson & Ericson (2005)	95°C – 5 min
	Reverse	myo3	CGGAAGAGCTCCAGGGCCTT		95°C – 40 sec 60°C – 40 sec 72°C – 1 min 25 cycles
	Reverse	myo3F*	GCAAGGACCTTGATAATGACTT		72°C – 8 min
RAG-1	Forward	RAG1_F	TTGAAAAAACACCCTCDGATG	Groth and Barrowclough (1999)	95°C – 5 min
	Reverse	RAG1_R	GTTGTTTCCACTGGATCTGCC		95°C – 40 sec 64°C – 40 sec 72°C – 1 min 35 cycles
	Reverse	RAGintR3*	TTAGCTGAGCACGTTCCCC	this study	72°C – 8 min

enberg Natural History Collections Dresden. DNA from toe pads was extracted using the sbeadex® forensic kit (LGC Genomics). Extraction was performed according to the manufacturer's instructions except for overnight incubation of tissue with proteinase K (instead of one hour) and only 60 µl elution volume (instead of 100 µl) in order to yield a sufficiently high concentration of DNA extracts. All toe pad samples were analyzed in a separate clean lab. There, each step of analysis (sampling, extraction, and PCR) was done on separate working benches. In order to avoid cross-contamination working benches were cleaned with DNA-away (Molecular Bio Products, Inc.) and after each step both benches and lab rooms were decontaminated with UV-light for at least four hours.

Marker choice: We amplified and sequenced the three markers used by Pasquet *et al*. (2014) for optimal comparison with their multi-locus data set: two mitochondrial genes (cytochrome *b* [cyt *b*] and cytochrome oxidase subunit I [COI]) and the nuclear RAG1. In addition, we sequenced the mitochondrial NADH dehydrogenase subunit 2 (ND2) for comparison with the data set by Zink *et al*. (2006) for *S. europaea*, and a further nuclear marker, intron 2 of the nuclear myoglobin gene (myo).

For all markers we applied PCR protocols from Päckert *et al*. (2015) except for RAG1 for which we used the PCR protocol by Groth & Barrowclough (1999; as cited in Pasquet *et al.*, 2014; for primers and other details see Table 1). PCR products were purified using ExoSap-IT (GE Healthcare; adding 0.1 µl ExoSap-IT solution in 4 µl H_2O to each sample; 37 °C for 30 min, 94 °C for 15 min). The sequencing of the PCR products was performed with BigDyeTM 3.1 Dye Terminator Cycle Sequencing Kits (Applied Biosystems), according to the manufacturers' instructions. Cycle sequencing products were purified by salt/ethanol precipitation or by using Sephadex (GE Healthcare, Munich, Germany), and sequenced in both directions on an ABI 3130xl DNA sequencer.

Historical toe pad samples were processed with Next-Generation-Sequencing (NGS) laboratory methodology in the clean-room facility at Senckenberg Dresden (Fulton, 2012) due to the highly fragmented nature of their DNA. This involved DNA extraction with the DNeasy Blood & Tissue Kit (Qiagen) and subsequent conversion of the template into double-stranded single-indexed Illumina sequencing libraries according to Meyer & Kircher (2010). In order to minimize sequencing costs, we

Table 2. Read and assembly information for historic toe pad samples (catalogue number and year of collection indicated) processed by NGS techniques.

taxon	cat no	year	raw reads	clean reads	COI	ND2	cytb	RAG1	myo	ODC
S. castanea	C56854	1968	286,730	189,066	+	+	+	5 wobbles	4 wobbles	10 wobbles
S.castanea	C60502	< 1960	252,084	174,145	+	+	+	+	1 wobble	+
S. cinnamoventris	C46283	1872	338,966	219,504	+	+	+	+	1 wobble	1 wobble
S.cinnamoventris	C46284	< 1900	261,568	190,044	+	+	+	2 wobbles	1 wobble	+
S. victoriae	C46278	1938	342,477	207,623	+	+	+	+	+	+

Table 3. Partition schemes and substitution models; as estimated with PartitionFinder.

	BEAST 1			BEAST 2			RAxML		
partition	**marker**	**codon**	**model**	**marker**	**codon**	**model**	**marker**	**codon**	**model**
1	Cytb + ND2	1	GTR + I + Γ	Cytb	All	GTR + I + Γ	Cytb + ND2 + COI	1	GTR + I + Γ
2	Cytb + COI	2	HKY + I + Γ	ND2	All	GTR + I + Γ	Cytb + ND2 + COI	2	GTR + I + Γ
3	Cytb	3	GTR + Γ	COI	All	GTR + I + Γ	Cytb	3	GTR + Γ
4	ND2	2	HKY + I + Γ	Myo	—	HKY + I + Γ	ND2 + COI	3	GTR + Γ
5	ND2 + COI	3	GTR + Γ	RAG1	All	GTR + Γ	Myo + RAG1	—	GTR + Γ
6	COI	1	TrN + I + Γ						
7	Myo	—	TrNef + Γ						
8	RAG1	1 + 2	HKY + Γ						
9	RAG1	3	TrNef + Γ						

performed two-rounds of in-solution hybridization capture to enrich the libraries for the targeted mitochondrial and nuclear loci (MARICIC *et al*., 2010; HORN 2012), using DNA baits generated from PCR products of *S. cashmirensis* and *S. himalayensis*. PCR conditions and primer sequences were the same as for fresh material. The enriched libraries were sequenced in-house on an Illumina MiSeq sequencing platform generating 75 bp paired-end reads. Assembling the individual loci involved adapter trimming with SKEWER v0.2.2 (JIANG *et al*., 2014), read merging (min. length 30 bp), quality filtering (min. Q-score 20), and duplicate removal with BBMAP-SUITE 37.24 (https://sourceforge.net/projects/bbmap/), before subjecting the readpools to a two-step baiting and iterative mapping approach in MITOBIM (HAHN *et al*., 2013) with an allowed mismatch value of 2. Resulting scaffolds were visualized and checked for assembly artifacts and sufficient coverage in Tablet (MILNE *et al*., 2013). After assembly, PCR priming sites were removed from amplicon assemblies and coding loci checked for internal stop codons in MEGA 7 (KUMAR *et al.*, 2016). For further read and assembly information see Table 2.

Sequence analysis

We aligned forward and reverse Sanger sequences for each gene by CLUSTALW using MEGA 5.1 (TAMURA *et al*., 2011) and we cross-checked the respective electropherograms with CHROMAS v.2.6.5 (Technelysium Pty Ltd) for possible inaccuracies due to sequencing or reading errors. For each marker per sample, we manually combined sequences of both reading directions to a single consensus sequence. All sequences used for analysis were deposited at GenBank or to European Nucleotide Archive (ENA) (Table S1). For comparison with our own sequences we used the nuthatch sequence data sets by PASQUET *et al.* (2014), PRICE *et al.* (2014), ZHAO *et al*. (2019) (all listed in Table S1) and single-locus data sets (ND2) from ZINK *et al*. (2006) (GenBank accession numbers DQ219499–219780) and from CHEN *et al.* (2019) (GenBank numbers MK203427-MK203487). The Certhioidea tree was rooted by two distantly related outgroups, the Bohemian Waxwing, *Bombycilla garrulus*, and the Goldcrest, *Regulus regulus*.

We used the ND2 data set (n = 154 sequences; including sequence data from ZINK *et al*., 2006, and CHEN *et al.*, 2019) for reconstruction of a statistical parsimony network with TCS v1.21 (CLEMENT *et al.*, 2000). For visualization of the network from TCS output files we used the online software tool TCSBU (SANTOS *et al*., 2016).

The multi-locus data set comprised a total of 3848 base pairs of five genetic markers: cyt *b* (964 bp), ND2 (899 bp), COI (614 bp; mtDNA in total = 2477 bp), myo (670 bp) and RAG1 (701 bp; nuclear markers in total = 1371 bp). We used PARTITIONFINDER v1.1.1 (LANFEAR *et al*. 2012) to estimate the best-fitting partitioning scheme and substitution models for phylogenetic reconstruction with BEAST and RAXML separately using the "greedy" search algorithm. The best schemes were determined to be a nine partition scheme for BEAST analysis and a five partition scheme for RAXML analysis (Table 3).

Phylogenetic relationships were reconstructed using maximum likelihood with RAXMLGUI v. 1.3 (STAMATAKIS, 2006; Silvestro & Michalak, 2012) and Bayesian inference with BEAST 1.8.1 (DRUMMOND & RAMBAUT, 2007). Maximum-likelihood bootstrap support was obtained by 1000 thorough bootstrap replicates with RAXML. For Bayesian

inference of phylogeny we performed three independent runs with BEAST for 50,000,000 generations (trees sampled every 5000 generations) under the uncorrelated lognormal clock model for all loci with the "auto-optimize" option activated and a Yule prior applied to the tree.

For inference of divergence time estimates, we used two different approaches. First, we used a fossil age constraint for the common ancestor of Certhioidea represented by *Certhiops rummeli*, the oldest known fossil from this superfamily that was described from the karstic early Miocene deposits near Eichstätt, Germany (MANEGOLD, 2008). The corresponding fossil age of 18–20 Ma had already been used for molecular dating of the entire Passeriformes tree (ERICSON *et al.*, 2014; CLARAMUNT & CRACRAFT, 2015) and of the nuthatch phylogeny by PASQUET *et al*. (2014). We performed our calibration according to the standard outlined by BENTON *et al*. (2009) who recommended the use of a soft maximum and minimum constraint that correspond to the oldest certain and the oldest possible date of origin of a clade. According to this approach, CLARAMUNT & CRACRAFT (2015: Fig. 1) had generated clade age priors for time calibration. Therefore we used their tmrca priors for Certhioidea (forced to be monophyletic) for our fossil calibration: zero offset = 18.0, Log(mean) = 2.0, Log(stdev) = 1.2 (thus the known fossil age 18-20.5 Ma covered the time interval from the zero offset to the maximum of the lognormal prior distribution (see BENTON *et al*., 2009: Fig. 2; CLARAMUNT & CRACRAFT, 2015: Fig. 1).

Second, as an alternative to the fossil-dating approach we applied a molecular clock calibration using mean substitution rate estimates for mtDNA markers such as the frequently applied cyt *b* rate of 0.0105 substitutions per site per lineage per million years (WEIR & SCHLUTER, 2008). For the nuthatch phylogeny we first relied on mean rates for our three mitochondrial genes as estimated by LERNER *et al*. (2011): cyt *b* = 0.014; COI = 0.016; ND2 = 0.029 (all values in substitutions per site per lineage per million years). Because each of these mean estimates referred to the entire gene including all three codon positions, we did not apply these mean rates to the eight-partition scheme but to a five-partition scheme treating each mitochondrial marker as one partition. Best-fit substitution models for the five partitions were estimated using MRMODELTEST v2 (NYLANDER, 2004) (Table 3). However, we compared divergence times resulting from this approach with an independent run under modified settings for parameter 'partition into codon positions' with '3 partitions'.

Third, we applied a mean rate for the 3rd codon position of all mitochondrial genes to partitions 3 (cyt *b* 3rd codon position) and 5 (COI and ND2 3rd codon position) of the nine-partition scheme (Table 3). That mean rate of 0.0361 substitutions per site per lineage per million years was estimated by QUILLFELDT (2017); we chose the rate for Passeriformes inferred from calibration 4 (see ALBRECHT *et al*. 2020 for further justification).

We used LOGCOMBINER v.1.8.1 to combine log files and tree files from independent runs with BEAST and we checked the combined log file in TRACER v. 1.4 (RAMBAUT & DRUMMOND 2007) to ensure adequate ESS files for all parameters (all ESS > 207). Consensus trees from both analyses were visualized in FIGTREE 1.3.1 (RAMBAUT, 2009).

Biometry

For comparison of body and feather dimensions we measured ten morphological traits for a total of 315 whole skins of all nuthatch species included in the phylogenetic analysis except *Sitta magna* of which we could not receive any specimens. The focus of the biometric analysis was set on the Eurasian nuthatch, *Sitta europaea*, of which we measured a total of 157 specimens (comprising 16 out of 20 currently accepted subspecies; all measurements taken by B.K.). Material from the following three bird collections has been examined: Museum of Zoology, Senckenberg Natural History Collections Dresden (MTD), Zoological Research Museum Alexander Koenig Bonn (ZFMK), and Museum für Naturkunde Berlin (MFN). Measurements were taken according to the standards in ECK *et al.* (2011) for: total body length (TL1), bill length (bill-to-skull, BSk), bill height (Bp) and bill width (BWp), wing length (maximum chord, Wmax), Kipp's distance (Kipp: distance between longest primary and first secondary; ECK *et al*. 2011), tail length (T1), tarsus length (Tar2), length of hind toe (dToeh) and length of hind claw (dCl). All measurements were taken by B.K. using a standard ornithological ruler for wing and tail parameters (15 cm/6 in; Ecotone) and a digital caliper (digiMax; Ecotone, Poland) with an accuracy of 0.01 mm for beak and tarsus dimensions. All measurements were taken under a magnifier lamp (Waldmann RLL 122T, magnification (lens: 120 mm diameter/ 4 diopters) to achieve maximum precision.

For within- and among-species comparison we performed principal component analyses (PCAs) for reducing the dimensionality of the morphological traits used. The final aim was to obtain few uncorrelated variables explaining the largest amount of variation. We applied this analysis for data sets including (i) all specimens of *Sitta europaea*, and (ii) all specimens of putative closest relatives of the Eurasian nuthatch, i.e the *S. castanea* group and allies (*S. nagaensis, S. cashmirensis, S. castanea*, *S. cinnamoventris,* and *S. neglecta*), and (iii) five species that occur in parapatry along an elevational gradient in the Central Himalayas. We used Levene's tests to confirm homoscedasticity and graphical tests for normality of variables. For the two first components, we performed subsequent ANOVA analyses (with Tukey post-hoc tests) to test for significant morphological differences within *Sitta europaea* phylogroups and the Asian parapatric species. We used a Bonferroni correction (0.05/test numbers) to avoid type I error. All analyses were performed with the programme R (Version 3.5.1; R CORE TEAM, 2018). PCAs were performed using the function "prcomp" and plots were obtained using the package "ggplot2" (WICKHAM, 2016).

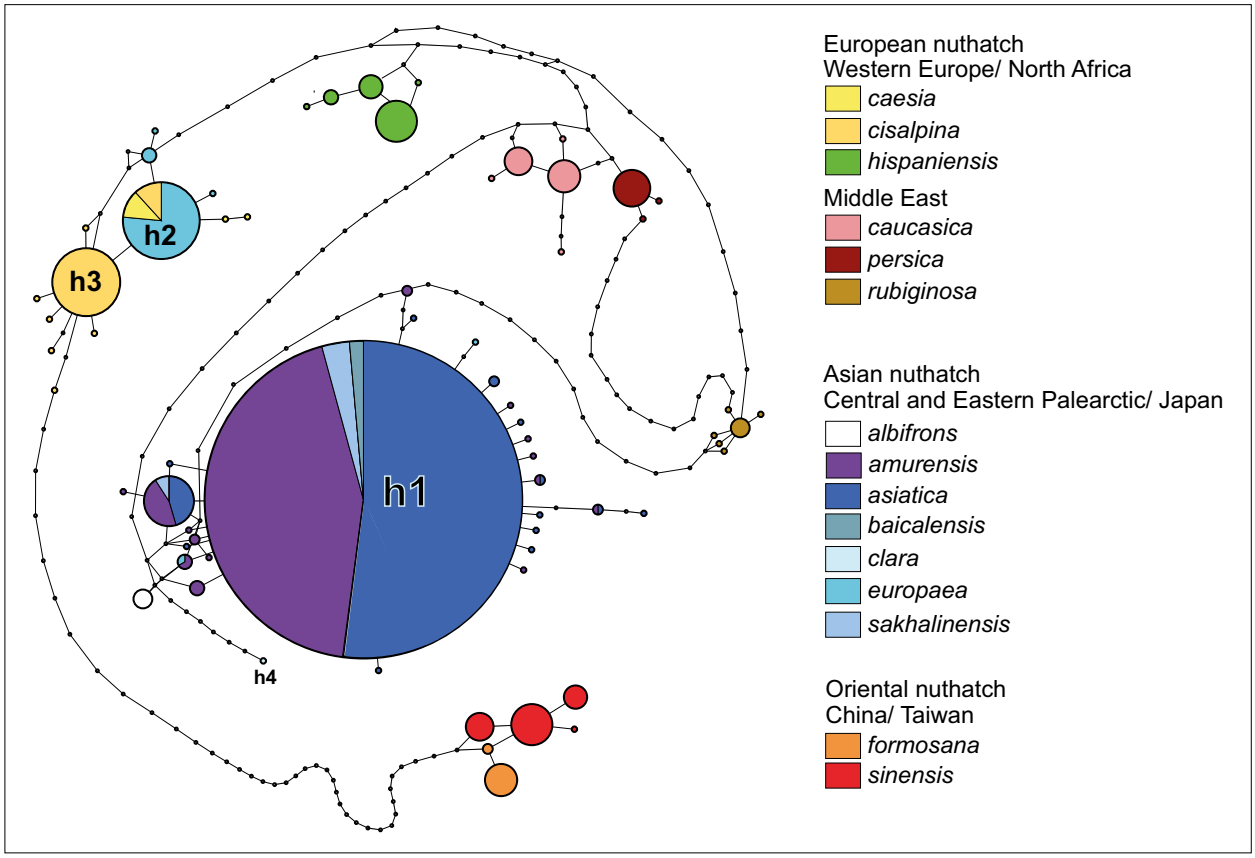

Fig. 2. Phylogeographic patterns within and among the three subspecies groups of the Eurasian nuthatch, *Sitta europaea* (subspecies affiliation of samples/haplotypes indicated by color code); statistical parsimony network of ND2 sequence data (637 bp; $n = 249$: own data plus published sequence data from ZINK *et al*. 2006 and from CHEN *et al*. 2019).

Results

Molecular genetics

Mitochondrial DNA – three phylogroups of *S. europaea*

The statistical parsimony network based on mitochondrial ND2 sequences is shown in Figure 2. A large Central and Eastern Palearctic cluster of the Asian nuthatch phylogroup showed a starlike structure with most haplotypes derived from a central one that was found in 71 individuals distributed from Scandinavia in the West across the entire taiga belt to Sakhalin in the East. Only subspecies *S. e. albifrons* from Kamtchatka and *S. e. clara* from Hokkaido (Fig. 2, h4) appeared as slightly differentiated tip haplotypes. The Japanese lineage differed from its continental counterparts from central and eastern Siberia by a minimum of eight substitutions (to *S. e. albifrons*; ten substitutions to the central haplotype cluster; Fig. 2). Likewise, populations from Japan and the adjacent Kuril Islands appeared as a separate cluster in the minimum spanning network for COI (separated by a minimum of three substitutions from other continental members of Asian nuthatch phylogroup; Fig. S1). Strikingly, only a single specimen (from Finland) of the white-bellied *europaea* group was nested in the Central and Eastern Palearctic haplotype cluster.

The European nuthatch phylogroup was separated into four major mitochondrial lineages. The two most common haplotypes (out of thirteen) of a Central European cluster were shared by seventeen individuals (h2) and fifteen individuals (h3), respectively. Haplotype h3 is found only in populations of *S. e. cisalpina*, whereas h2 was found in brown-bellied *S. e.caesia* and *S. e. cisalpina* as well as in white-bellied *S. e. europaea* (Fig. 2; western haplotypes in populations from Sweden and from western Russia [Moscow and Kursk; from ZINK *et al*. 2006]). That Central European cluster was separated from a previously undetected mitochondrial lineage from the Iberian Peninsula and North Africa (*S. e. hispaniensis*) by a minimum of eight substitutions (Fig. 2). The populations from the Middle East were divided into two separate haplotype clusters: (i) subspecies *S. e. caucasica* and *S. e. persica* were closely related and differed by a minimum of three substitutions, (ii) subspecies *S. e. rubiginosa* represented a cluster of its own that was separated by a minimum of seventeen substitutions from *S. e. persica* (Fig. 2).

Populations of the Oriental nuthatch phylogroup from continental China and Taiwan appeared as a highly diverged haplotype cluster (compare the distinctiveness of that lineage in the COI network; Fig. S1). Continental

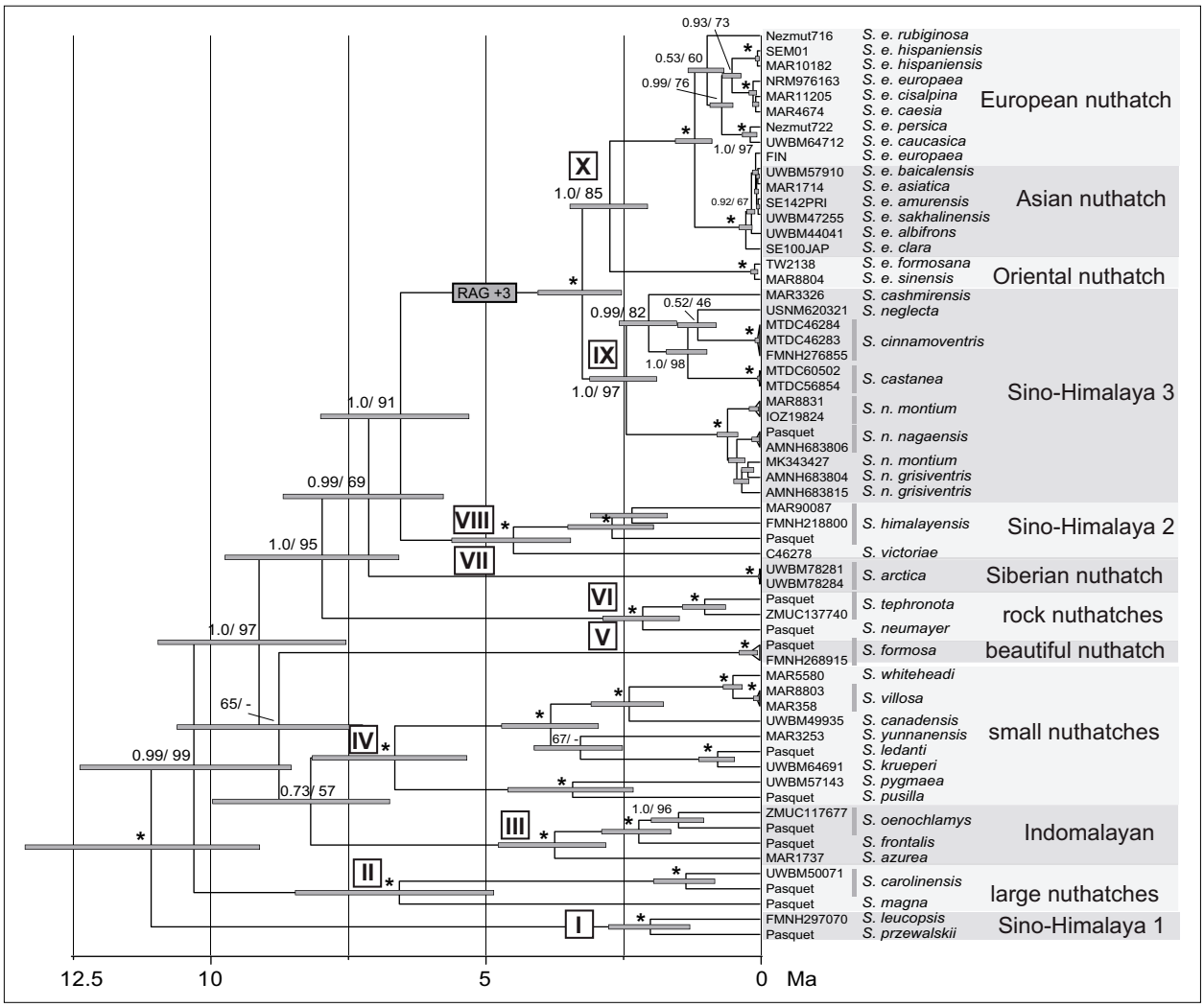

Fig. 3. Time-calibrated multi-locus phylogeny of nuthatches (*Sitta*; outgroups of other Certhioidea not shown); markers: cyt *b* (964 bp), ND2 (899 bp), COI (614 bp), myo (670 bp), RAG1 (701 bp); support values from Bayesian posterior probabilities/ likelihood bootstrap shown at nodes, * = full support from both analyses.

S. e. sinensis and *S. e. formosana* from Taiwan did not share any of the six haplotypes (Fig. 2).

Multi-locus phylogeny – a revised nuthatch tree

The multi-locus phylogeny based on two mitochondrial and two nuclear genes (see above) of *Sitta* nuthatches is shown in Fig. 3. The whole genus *Sitta* forms a well-supported monophyletic clade opposed to another poorly supported clade that included all remaining families of Certhioidea (Fig. 4A, B). Tree topologies inferred from BEAST and from RAXML were largely congruent.

Tree topology: We distinguished ten major phylogenetic clades of *Sitta* (Fig. 3, clades I to X). The Eurasian nuthatch, *S. europaea*, resulted as a strongly supported terminal clade (Fig. 3, clade X) that was divided into three larger and deeply split subclades. The brown-bellied Oriental nuthatch phylogroup was sister to a terminal clade uniting white-bellied forms of the Asian nuthatch phylogroup and brown-bellied forms of the European nuthatch phylogroup as two separate subclades (Fig. 3). Monophyly of the European nuthatch phylogroup, i.e. the basal position of Iranian *S. e. rubiginosa* was only poorly supported; however, the sister clade of *S. e. rubiginosa* received strong support and united three major subclades: (i) Caucasian and south Iranian *S. e. caucasica* and *S. e. persica*, (ii) Iberian and North African *S. e. hispaniensis,* and (iii) western and south-eastern European *S. e. caesia* and *S. e. cisalpina* plus one *S. e. europaea* from Sweden (Fig. 3).

The closest relatives of the Eurasian nuthatch, *S. europaea*, formed a monophyletic clade uniting five species from the Sino-Himalayas (Fig. 3, clade IX). The pale-bellied *S. nagaensis* and *S. cashmirensis* were successively basal to a terminal clade of three intensely brown-bellied species *S. castanea*, *S. cinnamoventris,* and *S. neglecta* (for their distributions compare Fig. 1B). Sister-group relationship of clades IX and X was furthermore supported by a shared 3-bp insertion in the RAG1 sequence resulting in a duplication of one glutamine in the amino acid sequence (Fig. 3).

The entire circum-Tibetan group of clades IX and X was sister to another species pair with disjunct distributions in the Himalayas, *S. himalayensis*, and in the Burmese Chin Hills, *S. victoriae* (Fig. 3, clade VIII). Strikingly, a deep split between three specimens of *S. himalayaensis* equaled interspecific divergences among species of clade IX (Fig. 3).

The Siberian nuthatch, *S. arctica*, (Fig. 3, clade VII) resulted as the sister of the entire crown clade of subclades VIII to X. Divergence time estimates for the split from its closest relatives ranged between a minimum estimate of 7.1 [5.6–8.7] Ma based on the fossil calibration to a maximum estimate of 13.1 [9.9–17.0] Ma based on the rate estimate for the 3rd codon position.

The rock-nuthatches, *S. tephronota* and *S. neumayer* (Fig. 3, clade VI), were sister to a monophyletic group uniting clades VII to X. These two large species from dry and more or less tree-less areas of the eastern Mediterranean and the Near East represent a rather specialized group living predominantly on rock faces.

Phylogenetic relationships of the beautiful nuthatch, *S. formosa,* the eastern Himalayas and adjacent Southeast Asia were equivocal: It was sister to the latter monophyletic group uniting clades VI to X in the RAXML tree with poor support (not shown) and sister to a monophyletic group uniting clades II and IV in the BEAST tree (Fig. 3; again with poor support). Clade III comprised three tropical species from the Indo-Malayan Region that are characterized by bright blue plumage, a distinct bare eye-ring, and colorful red or yellow bills. In this clade *S. azurea* from the Greater Sundas was sister to a terminal species pair of *S. frontalis* (from sub-Himalayan areas and India to the Greater Sundas) and *S. oenochlamys* (from the Philippines). These Indo-Malayan nuthatches were sister to a clade IV that comprised rather small nuthatches species that live in disjunct areas in Europe, the Near East, China, and in North America, respectively. Clade IV was divided in a Nearctic sister species pair (*S. pusilla*, *S. pygmaea*) and a terminal clade comprising five species from the Palearctic and one from the Nearctic (Fig. 3).

The two most ancient offshoots of the *Sitta* tree (Fig. 3) were clade II that united two rather large-bodied species from Asia, *S. magna*, and from North America, *S. carolinensis* and clade I that included the species pair *S. leucopsis* and *S. przewalskii*, both inhabiting temperate mountainous areas of the western Himalayas to Afghanistan and southwest China, respectively.

Divergence time estimates: We found a strong deviation between divergence times inferred from the fossil calibration and those based on mean rate estimates for mitochondrial markers. Generally, the fossil calibration yielded younger ages (e.g. 20.1 Ma [18.1–23.4 Ma] for the root age of Certhioidea; Fig. 4A), whereas oldest divergence time estimates were inferred from the clock calibration based on a mean estimate for the 3rd codon position of mtDNA markers (36.5 Ma [26.9–46.6 Ma] for Certhioidea Fig. 4B). The onset of the two radiations of clade X (*S. europaea*) and clade XI (Sino-Himalayan *S. castanea* group) ranged at similar dimensions with minimum divergence time estimates at the Pliocene-Pleistocene boundary (2.4–2.7 Ma; fossil-calibration) and maximum estimates in the early Pliocene (4.5–5.0 Ma; rate of 3rd codon position; Fig. 4C, D). Regardless of deviations among the different time-calibrations, the terminal split events in clades X and IX reflected an early to mid-Pleistocene origin of intraspecific East-West vicariance in the Northern Palearctic (*S. europaea*, clade X: fossil: 1.2 [0.9–1.6] Ma; rate 3rd codon: 2.2 [1.5–2.9] Ma) and in the Sino-Himalayas and adjacent Southeast Asia (intraspecific diversification of *S. nagaensis*; fossil: 0.6 [0.4–0.8] Ma; rate 3rd codon: 1.1 [0.7–1.5] Ma compare Fig. 3).

Morphology

According to phenotypical variation, generally two different phenotypes are distinguished in the Eurasian nuthatch, *S. europaea* (Fig. 5): brown-bellied forms (all subspecies of the European nuthatch and the Oriental nuthatch phylogroups) and white bellied subspecies of the Asian nuthatch phylogroup. Intermediate phenotypes of *S. europaea* with pale brownish underparts were found in Scandinavian, Baltic, and Eastern European populations (Figs 5E, S2) as well as in northeastern Chinese populations of *S. e. amurensis* (Fig. 5K, L).

Results from principal component analysis (PCA) of the biometric data set for *S. europaea* (n = 157 specimens) are shown in Figure 6A: The first principal component (PC1) had an eigenvalue of 2.0, explained 40.9% of the total variance, and was most heavily positively loaded by wing and tail lengths, and bill shapes (BSk, Bp, and BWp). The second component had an eigenvalue of 1.1 and explained a further 15.9% of the total variance (a cumulative 56.8% of the total variance). PC2 was most heavily negatively loaded by Kipp's distance and tail length, and positively loaded by hind claw and hind toe lengths. In the scatterplot of PC1 versus PC2 no clear clusters could be distinguished; however, body size dimensions showed clinal variation along the x-axis (PC1) with smallest individuals in the Oriental nuthatch phylogroup and largest in the European nuthatch phylogroup and *S. e. europaea* (Fig. 6A). Subsequent ANOVA analyses with PC1 showed significant differences among groups ($F_{4,126} = 57.85$, $p << 0.0001$). All post-hoc Tukey multiple comparisons were significant except between the Asian nuthatch and ssp. *amurensis* ($p = 0.374$). However, no significant differences were found with PC2 ($F_{4,126} = 2.61$, $p = 0.0386$).

The scatterplot from the second PCA for five species of the *S. castanea* group and allies showed a clustering of *S. cashmirensis* and *S. nagaensis* (Fig. 6B). The first component (PC1) had an eigenvalue of 1.96 explaining 42% of whole variation. It was most negatively loaded by wing length, Kipp's distance, and body length. The second component (PC2) obtained an eigenvalue of 1.51 and explained 22% (a cumulative 64%) of the total vari-

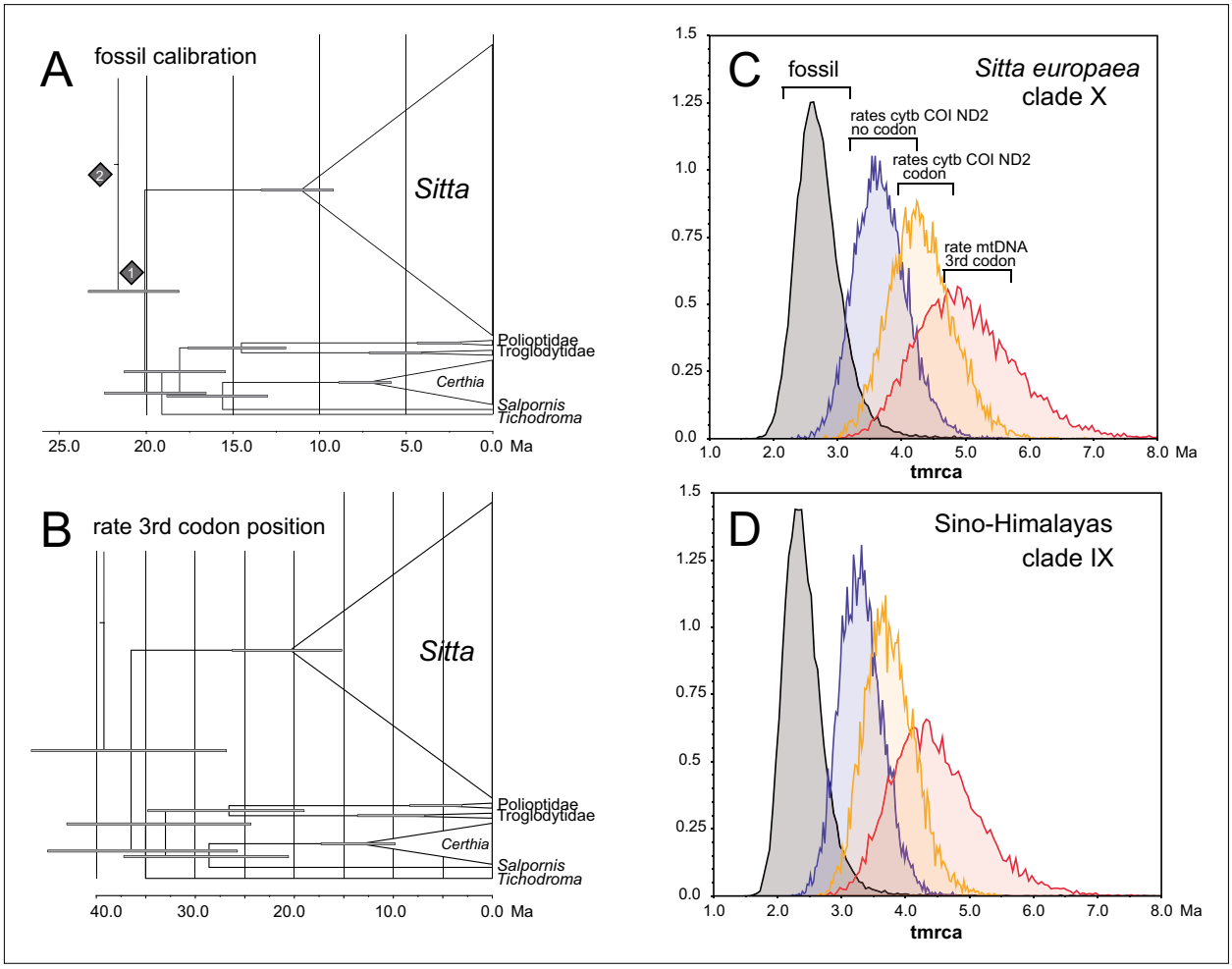

Fig. 4. Divergence time estimates for major clades of Certhioidea; **A**: fossil calibration; grey diamonds = constraint nodes: 1 = assuming the fossil *Certhiops* is nested in Certhioidea (our study; Ericson *et al.*, 2014; Claramunt & Cracraft, 2015), 2 = assuming the fossil represents the ancestor of all Certhioidea, thus providing a minimum age constraint for the root uniting Certhioidea and the outgroup (Oliveros *et al.*, 2019); **B**: inferred from a mean rate for the 3rd codon position of mitochondrial genes; times of the most recent common ancestor (tmrca), comparison of fossil dating and a molecular clock based on different mtDNA rates (marginal density plots inferred with TRACER) for: **C** = the Eurasian nuthatch, *S. europaea*; **D** = five species (*S. castanea*, *S. cashmirensis*, *S. castanea*, *S. cinnamoventris*, *S. nagaensis*) of the Sino-Himalayan sister clade IX of *S. europaea*; tmrca estimates inferred from (i) fossil calibration, (ii) mean rate estimates by Lerner *et al.* (2011) for cyt *b*, COI, and ND2 (blue: across all sites; yellow: partitioned by codon positions); a mean estimate of 0.0361 substitutions per site per lineage per million years for the 3rd codon position of mtDNA markers by Quillfeldt (2017; red).

ance. It was negatively loaded by hind toe length and bill height (Bp), and positively loaded by hind claw length. PC1 ANOVA showed significant differences ($F_{4,33} = 2.87$, $p = 0.038$). Post-hoc Tukey multiple comparisons showed that differences were only significant between *S. cashmirensis* and *S. nagaensis* ($p = 0.018$). ANOVA analyses performed with PC2 also showed significant differences ($F_{4,33} = 6.44$, $p < 0.001$). In this case, differences were significant between *S. cashmirensis* and *S. castanea* ($p = 0.002$), and between *S. castanea* and *S. nagaensis* ($p = 0.002$).

Finally, we performed a separate PCA for six species that occur along an elevational gradient in the Central Himalayas and in its forelands on the Indian Subcontinent (many of them with parapatric distributions; Fig. 7). PC1 had an eigenvalue of 2.21 and explained 52.5% of the total variation. It was most heavily loaded by wing length, body length, bill length, Kipp's distance, and tail length (decreasing parameter load). The second component had an eigenvalue of 1.26 and explained a further 13.8% (a cumulative 66.3%) of the total variance. It was negatively loaded by hind toe and hind claw lengths. Subsequent ANOVA analyses with PC1 showed significant differences among groups ($F_{5,36} = 15.23$, $p << 0.0001$). Post-hoc Tukey multiple comparisons showed that differences were significant between the two smallest species (*S. frontalis* and *S. himalayensis*; Fig. 7) and the remaining species ($p < 0.01$), but differences were not significant between *S. frontalis* and *S. himalayensis* ($p = 0.779$). ANOVA analyses performed with PC2 also showed significant differences ($F_{5,36} = 11.89$, $p << 0.0001$). Post-hoc Tukey multiple comparisons showed that differences were only significant between the high-montane species *S. leucopsis* and the remaining species ($p < 0.001$).

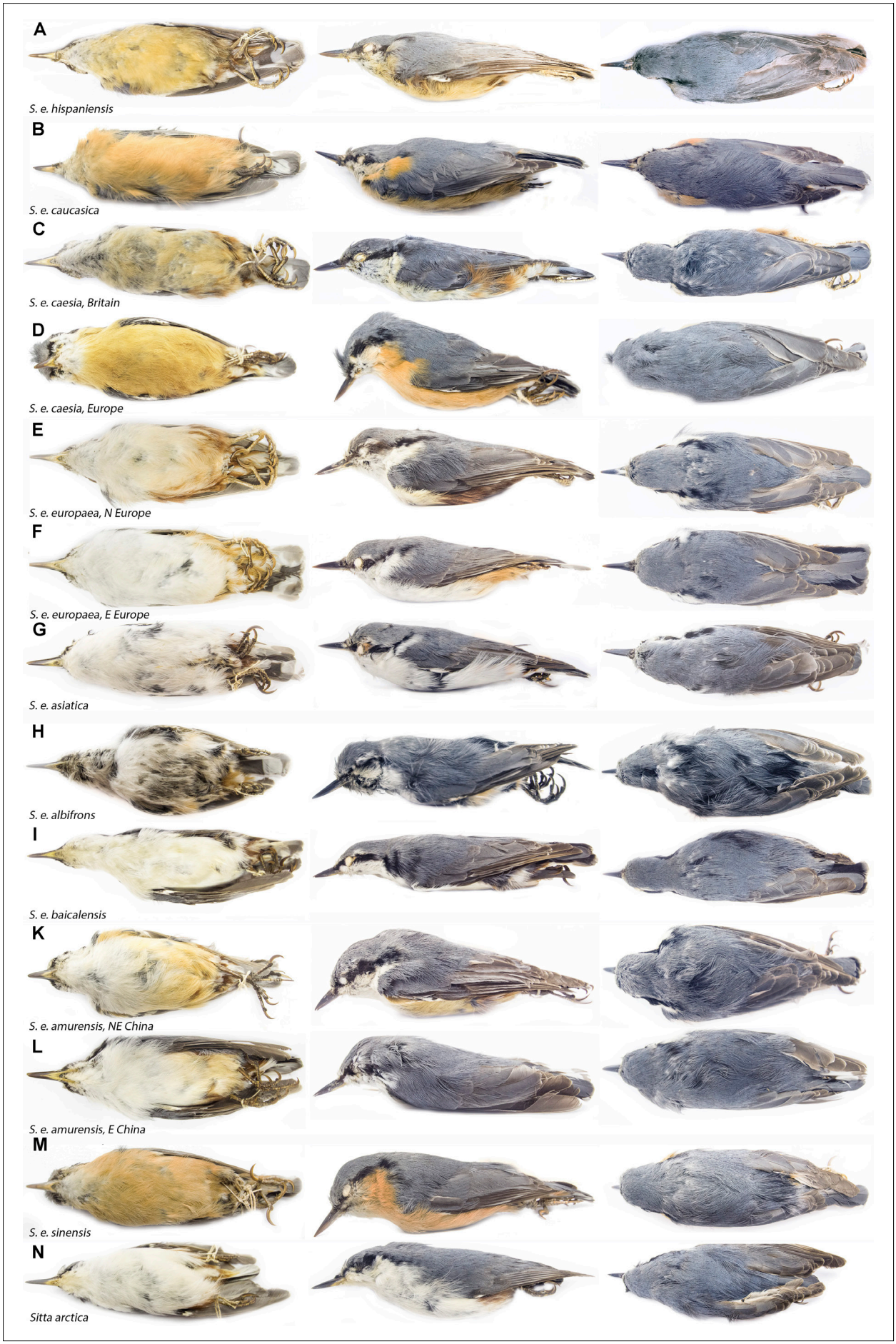
A
S. e. hispaniensis
B
S. e. caucasica
C
S. e. caesia, Britain
D
S. e. caesia, Europe
E
S. e. europaea, N Europe
F
S. e. europaea, E Europe
G
S. e. asiatica
H
S. e. albifrons
I
S. e. baicalensis
K
S. e. amurensis, NE China
L
S. e. amurensis, E China
M
S. e. sinensis
N
Sitta arctica

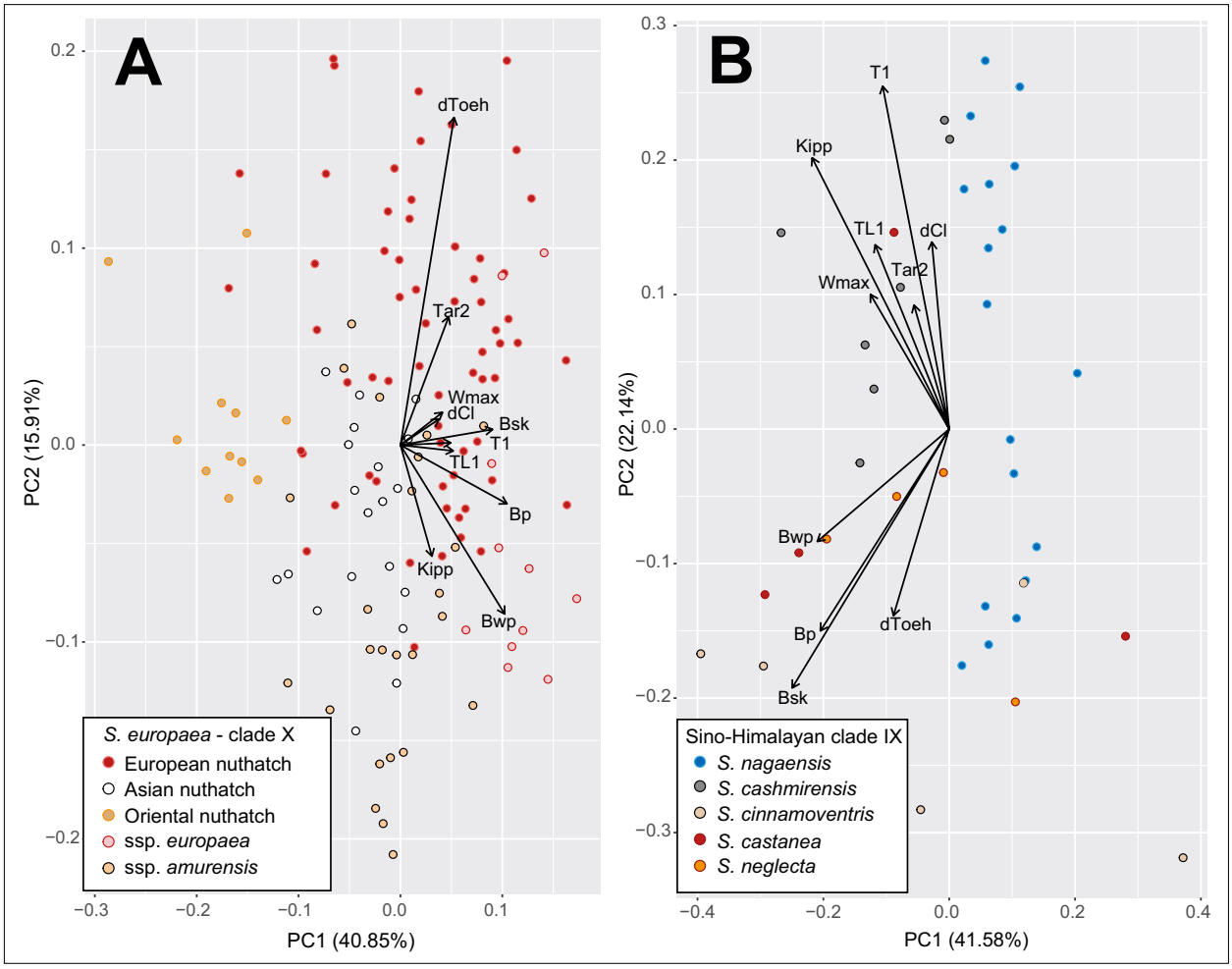

Fig. 6. Biometric differentiation of nuthatches from clades X and IX; scatterplots of principal components (PC) 1 and 2 from two separate analyses; **A**: the Eurasian nuthatch, *S. europaea*, clade X; colored dots distinguish between phylogroups (European nuthatch, Asian nuthatch, and Oriental nuthatch) and subspecies of intermediate phenotype between white-bellied and buff-bellied forms (*S. e. europaea*, *S. e. amurensis*); **B**: Sino-Himalayan species from clade IX.

Discussion

Tree topology and divergence time estimates

Tree topology of our nuthatch phylogeny reflects that by Pasquet's *et al*. (2014), however, we provide deeper insight in intra- and interspecific diversification of clades IX and X. Generally, our root age for Certhioidea of 20.1 Ma derived from the fossil calibration is in good accordance with split ages at the same node inferred from other fossil calibrations of the entire Aves tree (Davis & Page, 2014: 19 Ma; Moyle *et al*., 2016: 18 Ma). A mean age of approximately 23 Ma for Certhioidea was recently estimated by Oliveros *et al*. (2019) using thirteen avian fossils for calibration. This is striking in so far, as the latter authors had assigned the *Certhiops* fossil age to the node uniting Certhioidea and its sister clade (kinglets, Regulidae; compare our Figure 4A, calibration point 2). They compared six own calibrations (based on different settings) with four other time-calibrated phylogenies and all node ages for the Certhioidea-Regulidae split ranged between 25 and 30 Ma (in accordance with the younger root age of Certhioidea; compare Oliveros *et al*., 2019, their supplementary figures S6, S7).

More ancient root ages for Certhioidea were consistently inferred from our molecular clock calibrations based on empirical substitution rates of mtDNA markers (maximum age of 36.5 Ma based on the rate for the

← **Fig. 5.** Phenotypical differentiation of the Eurasian nuthatch, *S. europaea,* and the Siberian nuthatch, *S. arctica* (**N**); brown-bellied forms of the European nuthatch, *caesia* subspecies group (**A**–**D**); intermediate phenotype with pale brownish underpart, *S. e. europaea* from Norway (**E**); white-bellied forms of the Asian nuthatch, *europaea* subspecies group (**F**–**I**); intermediate phenotypes with pale brownish underpart, *S. e. amurensis* from northeastern and eastern China (**K**–**L**); brown-bellied *S. e. sinensis* (Oriental nuthatch, *sinensis* subspecies group; **M**); white-bellied, *S. arctica* (**N**).

3rd codon position). These divergence times rather correspond to the Certhioidea root age of 32 Ma estimated by Pasquet *et al*. (2014) who applied a combined rate-based and fossil-based time-calibration to their phylogeny, and to the divergence time estimate by Ericsson *et al*. (2014, suppl. 2/3: mean 37 Ma [27.8–47.0 Ma]). Though the latter authors also used *Certhiops rummeli* and five other fossils for their calibration, they applied a much broader tmrca prior interval to the Certhioidea node than for example Claramunt & Cracraft (2015). Thus, a cautious interpretation of divergence times is recommendable and we must consider that estimates derived from a fossil time-calibration could represent rather minimum split ages. In the following we discuss divergence-time estimates as time periods (between minimum and maximum estimates inferred from different time-calibrations).

Phylogroups of the Eurasian nuthatch, *Sitta europaea*

Strikingly, the three morphologically defined subspecies groups of *S. europaea* (Vaurie, 1959; Harrap & Quinn, 1996; del Hoyo & Collar, 2016) are in good accordance with three monophyletic phylogroups of our phylogeny (for intermediate forms and zones of intergradation, see next chapter).

Intraspecific diversification of *S. europaea* started during the Pliocene (5.0–2.8 Ma; early Pliocene according to mtDNA substitution rates, late Pliocene according to fossil-dating) when south-eastern populations of the Oriental nuthatch phylogroup split from ancestors of the entire Northern Palearctic branch. The Pliocene phase of climate cooling in Asia (a global trend that already started during the Miocene) was associated with two phases of intensified aridification of Central Asia and an eastward extension of the Chinese Loess Plateau at about 3.6 Ma and 2.6 Ma (Guo *et al*., 2004). There is evidence from the palynological record of the same time period of a strengthening contrast in Neogene vegetation between northern and southern China (~ 3–3.6 Ma; Jacques *et al*., 2013). The northernmost extension of late Miocene and Pliocene forest ecosystems (according to Wang *et al*., 2019) well coincides with a zoogeographic boundary in China at about 40° N that divides the Palearctic fauna in the North from the Sino-Japanese fauna in the South (Song *et al*., 2016). If the Neogene vegetation of northern China was indeed dominated by open grassland rather than by closed forest ecosystems (Wang *et al*., 2019) then the separation of the Oriental nuthatch lineage from its northern relatives was very likely enhanced by a break of a previously continuous Miocene forest belt.

In the North, later on during the early to mid-Pleistocene (regardless of the time calibration applied) the white-bellied forms of the Asian nuthatch phylogroup separated from the brown-bellied forms of the European nuthatch phylogroup. Pleistocene origin of East-West vicariance in the Northern Palearctic is a characteristic phylogeographic pattern that is paralleled in a number of Eurasian forest-dwelling passerines such as corvids (Haring *et al*., 2007, 2012; Zhang *et al*., 2012; Kryukov *et al*., 2004, 2017; Song *et al*., 2018) and tits (Kvist *et al*., 2003; Päckert *et al*., 2005; Tritsch *et al*., 2017). The far more diversified western phylogroup (European nuthatch *sensu* del Hoyo & Collar, 2016) occupies a broad range from North Africa in the Southwest all across Western and Southern Europe to the Caucasian region in the East (Voous & van Marle, 1953; Glutz von Blotzheim & Bauer, 1993). Apart from the two known mitochondrial lineages from Western Europe and the Caucasus we found that Iberian and North African *S. e. hispaniensis* represented a third so far undetected haplotype cluster. The Iberian Peninsula is one of the major Southern European glacial refugia (Hewitt, 2000, 2004; Schmitt, 2007) where a number of endemic taxa (both at the subspecies and species level) have diverged from their closest relatives in the Central and Northern Palearctic (*Phylloscopus ibericus*: Helbig *et al*., 1996; *Picus viridis*: Pons *et al*. 2011, 2019; *Sylvia inornata*: Brambilla *et al*., 2008; *Cyanopica cyanus*: Song *et al*., 2018; *Troglodytes troglodytes*: Albrecht *et al*. 2020).

Genetic distinctiveness of Caucasian populations has been described in other passerine species, too (*Phylloscopus sindianus*: Helbig *et al*., 1996; *Troglodytes troglodytes*: Drovetski *et al*., 2004; *Saxicola torquatus*: Zink *et al*., 2009; *Periparus ater*: Tietze *et al*., 2011). In *S. europaea* the strong diversification into three mitochondrial lineages in the Middle East is a rather unexpected pattern (Alborz, Zagros, and Caucasus clades in Nazarizadeh *et al*., 2016; Chen *et al*., 2019). Strikingly, we found another genetic split among Iranian populations at a similar level of genetic divergence in the eastern rock nuthatch, *S. tephronota*, between our sample from Daregaz (Khorasan; ZMUC137740; subspecies *S. t. obscura*) and a sample of unidentified origin from Pasquet *et al*. (2014). Mean split ages between these distinct Iranian clades inferred from fossil and rate-base time calibration ranged at 1.0–1.9 Ma (*S. tephronota*) and 1.0–1.8 Ma (Iranian *S. e. rubiginosa* vs. other *S. europaea* from the western clade), respectively. Whether the sample used by Pasquet *et al*. (2014) might be representative of one of the two other Iranian subspecies *S. t. dresseri* from the Zagros mountains or *S. t. iranica* from northeast Iran (Del Hoyo & Collar, 2016) requires further verification.

Finally, strong genetic distinctiveness of Chinese populations of the third phylogroup (Oriental nuthatch *sensu* del Hoyo & Collar, 2016; *sinensis* group) was already documented by Chen *et al*. (2019). Though variation of body size dimensions appeared to be rather clinal throughout the entire trans-Palearctic range of *S. europaea*, the Chinese forms (*S. e. sinensis*, *S. e. formosanus*) are smaller in all body size dimensions compared to their Northern Palearctic counterparts (Matthysen, 2010: Fig. 4). Again, this phylogeographic pattern is paralleled in many passerine sister taxa (at both the species and subspecies level) that replace each other in the Northern Palearctic and in southwest China (Martens *et al*.,

2011; Päckert *et al*., 2010, 2012). Comparison of ND2 sequences from Chen *et al*. (2019) identified northernmost records of *S. e. sinensis* from Beijing municipality (our *S. e. sinensis* samples originated from the same region) and southernmost records of *S. e. amurensis* in the Provinces Heilongjiang and Jilin). It seems that the postulated zoogeographic barrier in that region does not necessarily imply a sharp phylogeographic break, because Song *et al*. (2016) found several areas of local admixture between genetically distinct northern and southern populations of the same bird species. In fact, the same must be assumed for our nuthatch example as outlined in the following paragraph.

Zones of intergradation in *Sitta europaea*

The white-bellied Asian nuthatch phylogroup occupies a large distribution range from Japan, Sakhalin, and the Kurile Islands in the East across the entire Northern Palearctic taiga belt to southern Scandinavia, the Baltic States, western Russia, and Belarus. At both extremes of the range the white-bellied Central and Eastern Palearctic forms intergrade with each of the two brown-bellied forms of the *caesia* and *sinensis* phylogroups (Fig. 1A). These zones of intergradation were already roughly circumscribed by Voous & van Marle (1953; later modified and reprinted in Dickinson, 2006, and in Päckert *et al*., 2018). In the West a broad hybrid belt extends from Denmark across western parts of the Baltic Sea to the northern shores of the Black Sea. There, highly variable and locally distinctive hybrid forms exist that were previously subsumed under the name *S. e. homeyeri* Hartert, 1892, for Baltic populations and under *S. e. sztolcmani* Domaniewski, 1915, for populations from Eastern Europe. Both taxa are usually being synonymized with nominate *S. e. europaea* (Vaurie, 1959; Greenway, 1967) but their clear hybrid character was often emphasized (Domaniewski, 1917; Stresemann, 1919; Voous & van Marle, 1953; Red'kin & Konovalova, 2006). Already Zink *et al*. (2006) discovered introgression of western ND2-haplotypes (brown-bellied European nuthatch cluster) in phenotypically white-bellied birds (Asian nuthatch cluster, haplotype h3 in Fig. 2) even beyond the range of phenotypically intermediate "*homeyeri*" birds (Fig. 1A). However, our local and regional sample sizes are too small as to infer information on directionality of introgression and on the extent of the intergradation zone from our data. Generally, patterns of gene flow can be reliably inferred from nuclear markers only and could be an interesting research question for future studies.

In the East the northern range limits of the brown-bellied Oriental nuthatch (*sinensis* group) roughly correspond with the northern zoogeographic boundary between the Palearctic and the Sino-Japanese fauna postulated by Song *et al*. (2016). North of this line, phenotypically intermediate individuals with a variable amount of brownish tinge in the underparts have been recorded all across the range of *S. e. amurensis* and in *S. e. bedfordi* from Jeju Island in South Korea (drawing in del Hoyo & Collar, 2016). Red'kin & Konovalova (2006: Fig. 1) classified the latter two taxa in a 'rufous-bellied' subspecies group as opposed to the adjacent white-bellied forms in the North and 'rufous-breasted' forms in the South. For this Far Eastern form zones of intergradation have been described in the Amur Region (with white-bellied *S. e. baicalensis*) and in the South in north-eastern Hebei Province (with brown-bellied *S. e. sinensis*; del Hoyo & Collar, 2016). All distributional maps indicate only a short line of geographical contact between both subspecies east of the Gulf of Bohai, but their interactions seem to be undescribed. Voous & van Marle (1953) indicated a zone of hybridization in that area but give no explanatory details. Red'kin & Konovalova (2006) depict a contact line but no hybridization area. However, in our phenotypic analysis all specimens from the northern Chinese range of *S. e. amurensis* had a clear intermediate phenotype between white- and brown-bellied forms (compare Fig. 5). Del Hoyo & Collar (2016) state that *S. e. amurensis* and *S. e. sinensis* intergrade in a very narrow zone in northern Hebei. Future studies on the extent of putative gene flow between the Chinese and the Far Eastern populations are certainly needed.

Diversification and elevational parapatry in Sino-Himalayan nuthatches

Though the Eurasian nuthatch, *S. europaea*, does not penetrate into the Himalayas, its closest relatives have always been assumed in this region (see Weigold, 2005). In fact, the six Sino-Himalayan nuthatch species of clade IX started diversifying during the Pliocene (4.5-2.4 Ma) at the same time when east of the Tibetan Plateau ancestors of the Oriental nuthatch lineage separated from their Northern Palearctic counterparts (*S. europaea*, clade X). However, in the Sino-Himalayan mountain forests the situation was far more complex compared to that in the plain taiga forests of the Northern Palearctic, because already during the late Miocene ancestors of two further Sino-Himalayan nuthatch lineages must have occupied niche space at high elevations (large-sized ancestors of clade I) and at medium elevations (smaller-sized ancestors of clade VIII; Figs 3, 7). Yet, during the Pliocene phase of their Asian radiation three further nuthatch species of clade IX diversified in ecological segregation: (i) at higher elevations in the West from Afghanistan to west Nepal (*S. cashmirensis*) and (ii) in the Himalayan forelands (*S. castanea;* the plains group according to Harrap & Quinn, 1996), at low to mean elevations (*S. cinnamoventris*; the foothills group according to Harrap & Quinn, 1996). The onset of diversification coincides with a Pliocene peak of diversification of the Himalayan avifauna that according to Price *et al.* (2014) mainly occurred along the elevational gradient. The first characteristic East-West splits among Sino-Himalayan sister species already emerged during the Pliocene, too, i.e. the split among the Himalayan endemic *S. himalayensis*

and the Burmese endemic *S. victoriae*. Already Weigold (2005) correctly identified these as closest relatives.

However, the remaining phylogeographic East-West disjunctions in the Sino-Himalayas were dated to the Pleistocene as in many other passerine species pairs, too (Päckert *et al*., 2012, 2015). Pleistocene lineage separation gave rise to two further Sino-Himalayan nuthatch species pairs: *S. leucopsis* / *S. przewalskii* at high elevations (clade I) and *S. cinnamoventris* / *S. neglecta* at lower elevations (clade IX). Particularly at higher elevations there is evidence of multiple fragmented forest microrefugia at a maximum tree line up to 3500 m during the LGM (Opgenoorth *et al*., 2010 for juniper forests). In the Western Himalayas cyclic contraction and expansion of these forest microrefugia in warm and cold cycles went along with vegetation shifts from forest vegetation to *Artemisia* / chenopod/grass steppe (Behrensmeyer *et al*., 1992: p. 487) or from conifer forests (*Pinus* and *Abies*) to evergreen oak (*Quercus semecarpifolia*) and alder (*Alnus*) forests (Manish & Pandit, 2018).

However, despite Pleistocene fragmentation of the montane forest belt, most Himalayan glacial forest refuges must have harbored a high diversity of paleoforest vegetation as suggested from the palynological record. In the Central Himalayas, timberline shifted downhill during the late Pleistocene from about 3900 m to 2900 m (Paudayal & Ferguson, 2004; Manish & Pandit, 2018) – and accordingly nuthatches of clades I, III, VIII and IX would have followed that vegetation shift towards breeding ranges at lower elevations. Below an upper narrow belt of *Betula utilis* and *Abies spectabilis* forest between 2965 m and 2200 m temperate mixed oak forests extended from median elevations down to 980 m and below (Paudayal & Ferguson, 2004; Ranhotra *et al*., 2017).

Very likely the subtropical and tropical forest belts at the Himalayan foothills have been less fragmented than the temperate and boreal forest belts during the Pleistocene and facilitated faunal exchange with adjacent areas. For example, during the early Pleistocene *S. frontalis* split from its Indo-Malayan relatives (clade III) and must have colonized tropical rainforests and mixed deciduous forests of the Himalayan foothills (Martens & Eck, 1995; Harrap, 2008) at its northern range limits. As an Indo-Malayan faunal element *S. frontalis* is the only subtropical/tropical immigrant in Himalayan nuthatch communities. Thus, along with in-situ diversification (for example among species of clade IX) immigration must have contributed (to a minor degree) to the extant complexity of Sino-Himalayan nuthatch communities (compare Johansson *et al*., 2007; Päckert *et al*., 2012). Last, intraspecific diversification in allopatry could be confirmed for some of the Sino-Himalayan endemics, such as for *S. nagaensis* (Zhao *et al*., 2019).

Thus ecological segregation of nuthatch species along the elevational gradient in the Himalayas was established over a long period of their biogeographic history. This is what makes the Himalayan arc and its forelands an especially nuthatch-rich area. This includes the mountain systems of the Indo-Burmese Biodiversity Hotspot (Marchese, 2015) where regional species richness is highest due to a number of narrow-range endemics (such as *S. victoriae*, *S. neglecta*, *S. formosa* and *S. magna*).

Sitta arctica – an ancient subarctic relict

The taxonomic status and the systematic affiliation of the enigmatic Siberian nuthatch or taiga nuthatch, *S. arctica,* have long been debated. A recent phylogenetic study placed *S. arctica* as distant relative of *S. europaea* and three further Sino-Himalayan species without reliably resolving the phylogenetic relationships (Chen *et al*., 2019). Our phylogenetic reconstructions placed *S. arctica* as a rather ancient offshoot from a monophyletic assemblage of *S. europaea* and two further Sino-Himalayan species groups (Fig. 3, clades VIII-X; including eight currently accepted nuthatch species). Apparently, *S. arctica* separated from its closest relatives in the South as early as the late Miocene (7.1 Ma – 13.1 Ma) when during the Tortonian the first cold taiga forests emerged at high latitudes of the Palearctic (Finlayson, 2011; Pound *et al*., 2012). According to climate-vegetation modeling by Forrest *et al*. (2015) the far northeastern Palearctic was then dominated by boreal evergreen coniferous trees, whereas at lower latitudes the taiga forest belt and the Sino-Himalayan forest belt were composed of temperate broad-leaved deciduous trees. Thus, separation between *S. arctica* and ancestors of medium-sized montane nuthatch species of clades VIII, IX, and X was likely associated with adaptation to different climate regimes and forest ecosystems. Today, the breeding range of *S. arctica* stretches from the Yenisei River Basin and Yakutia across Anadyrland towards central and north-eastern Siberia where it overlaps with breeding areas of other eastern subspecies, such as *S. e. baicalensis* and *S. e. asiatica* (Red'kin & Konovalova, 2006; del Hoyo & Collar 2016). The Siberian nuthatch, *S. arctica*, therefore represents an ancient relict form endemic to the far northeastern Palearctic. As such, the Siberian nuthatch provides a quite singular example in Palearctic birds except, perhaps, the Siberian crane, *Leucogeranus leucogeranus*. This subarctic crane species is currently restricted to two widely allopatric breeding areas with the only larger extant population in Yakutia (del Hoyo & Collar, 2014), and represents the earliest late Miocene offshoot of the crane phylogeny (Krajewski *et al*., 2010).

Taxonomic implications

The Siberian nuthatch, *Sitta arctica*: Our results support the previously suggested species status of this taxon (Dickinson & Christidis, 2014; del Hoyo & Collar, 2016; Gill *et al*., 2020). It is neither nested in the Eurasian nuthatch, *S. europaea*, clade nor is it the sister to this widespread species as previously assumed (Zink *et al.*, 2006; del Hoyo & Collar, 2016). Lineage separation from its closest relatives dates back at least to the late

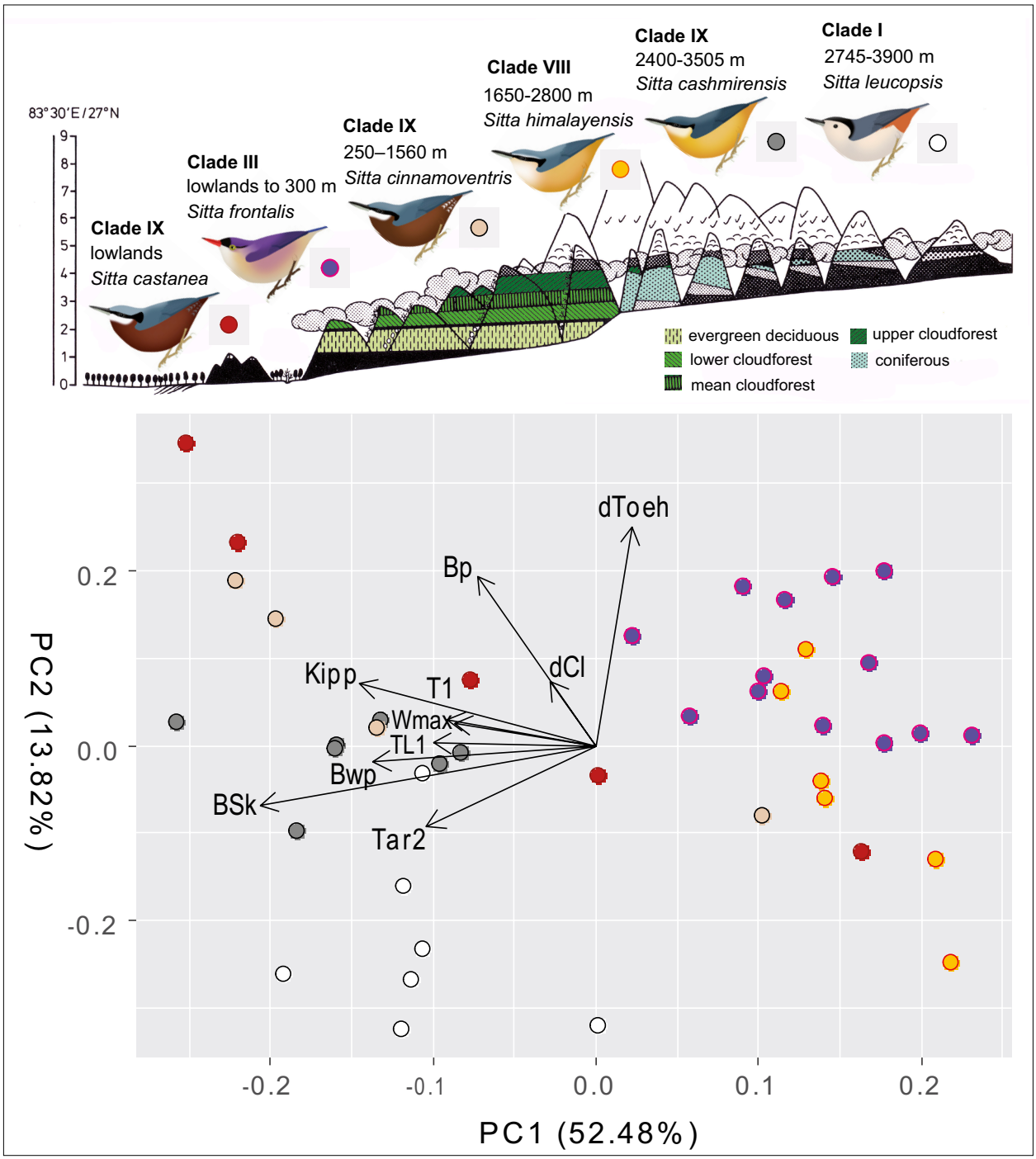

Fig. 7. Elevational parapatry of nuthatches in the Himalayas: Elevational profile modified from Martens & Eck (1995); nuthatch graphics by Totodu & L. Shyamal (2008); scatterplot of principal components 1 and 2 from PCA 2.

Miocene and it must be assumed that *S. arctica* is an ancient relict form that is separated from *S. europaea* with respect to habitat preference and behavior (vocalizations: Leonovich *et al*. 1996) across a still insufficiently defined range of sympatry. Based on multiple evidence from morphology and behavior, Eck (1984; 1996) already suggested species status for *S. arctica*. His diagnosis was later supported by biometric analyses (Red'kin & Konovalova 2006; Red'kin *et al*., 2016). Later taxonomists of the BOU Records Committee relating to the British List (Sangster *et al*., 2012) followed their recommendations.

In our biometric analysis, *S. arctica* was underrepresented and thus a lack of distinctiveness from the highly variable subgroups of *S. europaea* cannot be reliably inferred from our data. According to biometric analyses of broader sample sizes (Red'kin & Konovalova, 2006; Red'kin *et al*., 2016), differences between *S. arctica* and geographically adjacent *S. europaea* subspecies relate to larger body size, longer and thinner bill with plain culmen, shorter tarsometatarsus, and shorter hind toe (however, in *S. arctica* the claw of the hind toe is longer than in *S. europaea* and is as long as the toe itself). Also head

pattern differs with *S. arctica* having a shorter black eye stripe and a more prominent white supercilium, and lacking sexual dimorphism (as compared to *S. europaea*: Red'kin & Konovalova, 2006; Red'kin *et al*., 2016).

The Eurasian nuthatch, *Sitta europaea*: Zink *et al*. (2006) were the first to propose species status under the phylogenetic species concept (PSC) for the three phylogroups of *S. europaea* based on their phylogeny. Their classification relied on the criteria of diagnosability and reciprocal monophyly (Sangster, 2014) of the three proposed phylospecies though they did not take the entire subspecific variation into account. As soon as samples from zones of intergradations are included in the data set, the criteria of the PSC cannot be properly applied because introgression of the buff-bellied European nuthatch mitogenome into the white-bellied Asian nuthatch group causes gene tree paraphyly not only of the European nuthatch group but also of the nominate subspecies *S. e. europaea* Linnaeus, 1758 (Figs 1A, 2, 3). The latter taxon comprises very heterogeneous populations of white-bellied forms (from Scandinavia) but also pale buff-bellied forms from the East European intergradation zone (of subspecies *homeyeri* and *sztolcmani* that are currently synonymized with nominate *S. e. europaea*). Moreover, a proper assignment of species-level taxon names to either of the two terminal clades would require a clear and unambiguous assignment of *S. e. europaea* to only one of the two clades, because for reasons of priority it would be the nominate taxon for either of the two phylogroups.

The biospecies concept provides a different perspective on the wide trans-Palearctic range of the Eurasian nuthatch including at least two zones of secondary contact. First, there is evidence that the Eastern European zone of intergradation (including mitochondrial introgression between the Asian nuthatch and the European nuthatch phylogroups) is rather wide, though its spatial extent is less than roughly sketched and the degree and directionality of gene flow remain to be investigated. The same holds true for a putative eastern zone of intergradation between the Asian nuthatch phylogroup and the Oriental nuthatch phylogroup (phenotypically intermediate *S. e. amurensis*). Therefore, according to phenotypical diagnosis we might assume that the three phylogroups of *S. europaea* are connected by gene flow across rather wide zones of intergradation (unlike for example narrow hybrid zones with limited gene flow, e.g. in south-western Chinese areas of secondary contact in bushtits, *Aegithalos*: Wang *et al*., 2014). However, a confirmation from population genetic analysis is still lacking, thus for the time being we do not recommend a species-level split between the three phylogroups of *S. europaea*, despite rather high genetic distances.

The Sino-Himalayan sister clade (IX) of *S. europaea*: Currently, most authorities distinguish five species level taxa that were reflected as five separate subclades of clade IX (Fig. 3): *S. castanea*, *S. cashmirensis*, *S. cinnamoventris, S. nagaensis,* and *S. neglecta*. Interspecific divergence time estimates range at very similar levels like those between the three phylogroups of *S. europaea*, thus treating clade X as a single taxon while distinguishing five species of clade IX (at the same level of genetic divergence) seems inconsistent at first sight. Recognition of *S. nagaensis* is reasonable due to greatest within-clade divergence and for its wide-range sympatry with *S. neglecta* (Fig. 1B). Furthermore, lineage separation and divergence of phenotypes within clade IX was apparently associated with elevational niche segregation in the Himalayas and its forelands (e.g. between *S. cashmirensis*, *S. cinnamoventris*, and *S. castanea*; Fig. 7). Whether each of the three intensely brown-bellied parapatric taxa of clade IX (*S. castanea*, *S. cinnamoventris,* and *S. neglecta*) would merit species-level status is indeed debatable (see Greenway, 1969; Dickinson, 2006; Dickinson & Christidis, 2014). Like in the previous example, any justification of species splits in this complex phylogroup cannot be inferred from a time-calibrated phylogeny (even though based on a dense taxon-sampling) but must be based on range-wide ecological, behavioral, and population genetic analyses.

The white-cheeked nuthatch, *S. leucopsis*: This species has not been subject to comparative phylogenetic analyses before. It was treated conspecific with *S. przewalskii* until a species-level split of these two taxa was suggested based on morphology (Rasmussen & Anderton, 2005) and on marked vocal differences (Martens *et al*., 2011). Several taxonomic authorities followed that recommendation (del Hoyo & Collar, 2016; Clements *et al*., 2017; Gill *et al*. 2020). Mean split divergence time estimates between *S. leucopsis* and *S. przewalskii* correspond to those between other vicariant sister species of nuthatches, such as *S. neumayer* and *S. tephronota* or *S. pusilla* and *S. pygmaea*.

Acknowledgements

We are grateful to the following colleagues who provided sample loans for genetic analysis: S. Birks from Burke Museum of Natural History and Culture, USA (UWBM); J. Fjeldså from Zoological Museum of the University of Copenhagen (ZMUC), Denmark; C. Milensky from Smithsonian National Museum of Natural History, NY, USA; Guillermo López from IBICO in Spain; J.M. Pons from Muséum Nationale d'Histoire Naturelle Paris; H. Grimm and M. Fischer from Naturkundemuseum Erfurt and D.T. Tietze from Centrum für Naturkunde at Universität Hamburg contributed further samples to collection MAR at MTD Senckenberg Dresden. We thank Spanish and Moroccan authorities for providing sampling permits. Skins additional to those of the Dresden collection were studied in the collections of Zoological Research Museum Alexander Koenig, Bonn, and Museum für Naturkunde Berlin under the care of T. Töpfer and S. Frahnert, respectively. J. M. thanks Feldbausch Stiftung and Wagner Stiftung, both at Fachbereich Biologie of Mainz University, and Research commission of Deutsche Ornithologen-Gesellschaft (East Asia Grants

to J. Martens, A. Gebauer, and M. Kaiser) for travel grants. We received funding for pilot analysis from the research funding program "LOEWE-Landes-Offensive zur Entwicklung Wissenschaftlich-ökonomischer Exzellenz" of the Hessen State Ministry of Higher Education, Research, and the Arts. We received further funding for wet lab work from Deutsche Forschungsgemeinschaft (DFG), PA1818/3-1 and from UNESCO Bangkok under contract number 4500306550. YHS was supported by grants of the National Natural Science Foundation of China (30620130110), and JCI by a GRUPIN research grant from the Regional Government of Asturias (Ref.: IDI/2018/000151). Genetic work was conducted in the Senckenberg Dresden Molecular Laboratory (SGN-SNSD-Mol-Lab). We cordially thank all friends, colleagues and institutions.

References

Albrecht, F., Hering, J., Fuchs, E., Illera, J. C., Ihlow., F, Shannon, T. J., Collinson, M. J., Wink, M., Martens, J. & Päckert, M. (2020). Phylogeny of the Eurasian Wren *Nannus troglodytes* (Aves: Passeriformes: Troglodytidae) reveals deep and complex diversification patterns of Ibero-Maghrebian and Cyrenaican populations. *PLoS ONE*, **15**, e0230151.

Behrensmeyer, A. K., Damuth, J. D., DiMichele, W. A., Potts, R., Sues, H.-D. & Wing, S. L. (eds) (1992). *Terrestrial Ecosystems Through Time – Evolutionary Paleoecology of Terrestrial Plants and Animals*. Chicago & London, The University of Chicago Press.

Benton, M. J., Donoghue, P. C. & Asher, R. J. (2009). Calibrating and constraining molecular clocks, pp. 35–86 *in*: Hedges, S. B. & Kumar, S. (eds) *The Timetree of Life*. Oxford, Oxford University Press.

BirdLife International and NatureServe (2015). *Bird Species Distribution Maps of the World. Version 5.0*. Arlington, Texas, and Cambridge, BirdLife International, and NatureServe.

Brambilla, M., Vitulano, S., Spina, F., Baccetti, N., Gargallo, G., Fabbri, E., Guidali, F. & Randi, E. (2008). A molecular phylogeny of the *Sylvia cantillans* complex: cryptic species within the Mediterranean basin. *Molecular Phylogenetics and Evolution*, **48**, 461–472.

Campbell, K. K., Braile, T. & Winker, K. (2016). Integration of genetic and phenotypic data in 48 lineages of Philippine birds shows heterogeneous divergence processes and numerous cryptic species. *PLoS ONE*, **11**, e0159325.

Chapman, F. M. (1924). Criteria for the determination of subspecies in systematic ornithology. *The Auk*, **41**, 17–29.

Chen, Y.-H., Nazarizadeh, M., Lei, F.-M., Yang, X.-J., Yao, C.-T., Dong, F., Dong, L., Zou, F.-S., Drovetski, S. V., Liu, Y., Huang, C.-C. & Hung, C.-M. (2019). The niches of nuthatches affect their lineage evolution differently across latitude. *Molecular Ecology*, **28**, 803–817.

Claramunt, S. & Cracraft, J. (2015). A new time tree reveals Earth history's imprint on the evolution of modern birds. *Science Advances*, **1**, e1501005.

Clement, M., Posada, D. & Crandall, K. A. (2000). tcs: a computer program to estimate gene genealogies. *Molecular Ecology*, **9**, 1657–1659.

Clements, J. F., Schulenberg, T. S., Iliff, M. J., Roberson, Fredericks, D. T. A, Sullivan, B. L. & Wood, C. L. (2017). The eBird/Clements checklist of birds of the world: v2017. Downloaded from http://www.birds.cornell.edu/clementschecklist/download/ (accessed on 25 July 2018).

Cracraft, J., Barker, F. K., Braun, M., Harshman, J., Dyke, G. J., Feinstein, J., Stanley, S., Cibois, A., Schikler, P., Beresford, P., García-Moreno, J., Sorenson, M. P., Yuri, T. & Mindell, D. P. (2004). Phylogenetic relationships among modern birds (Neornithes), pp 468–489 *in*: Cracraft, J. & Donoghue, M. J. (eds) *Assembling the Tree of Life*. Oxford, Oxford University Press.

Davis, K. E. & Page, D. R. M. (2014). Reweaving the tapestry: a supertree of birds. *PLoS Currents*, **6**, doi: 10.1371/currents.tol.c1af68dda7c999ed9f1e4b2d2df7a08e (last accessed on 18 May 2020).

del Hoyo, J. & Collar, N. J. (Eds.) (2014). *Illustrated Checklist of the Birds of the World*. Volume 1 Non-Passerines. Barcelona, Lynx Edicions.

del Hoyo, J. & Collar, N. J. (eds) (2016). *Illustrated Checklist of the Birds of the World. Volume 2, Passerines*. Barcelona, Lynx Edicions.

del Hoyo, J., Elliot, A. & Christie, D. (eds) (2008). *Handbook of the Birds of the World. Volume 13 Penduline-tits to Shrikes*. Barcelona, Lynx Edicions.

Dickinson, E. C. (2006). Systematic notes on Asian birds. 62. A preliminary review of the Sittidae. *Zoologische Mededelingen*, **80,** 225–239.

Dickinson, E. C. & Christidis, L. (2014). *The Howard and Moore Complete Checklist of the Birds of the World. 4th Edition, Volume **2**: Passerines*. Eastbourne, Aves Press.

Domaniewski, J. v. (1917). *Sitta europaea homeyeri* Hart. und verwandte Formen. *Verhandlungen der Ornithologischen Gesellschaft in Bayern*, **13**, 174–180.

Dove, C. J., Rotzel, N. C., Heacker, M. & Weigt, L. A. (2008). Using DNA barcodes to identify bird species involved in birdstrikes. *Journal of Wildlife Management*, **72**, 1231–1236.

Drovetski, S. V., Zink, R. M., Rohwer, S., Fadeev, I. V., Nesterov, E. V., Karagodin, I., Koblik, E. A. & Red'kin, Y. A. (2004). Complex biogeographic history of a Holarctic passerine. *Proceedings of the Royal Society of London B, Biological Sciences*, **271**, 545–551.

Drummond, A. J. & Rambaut, A. (2007). beast: Bayesian evolutionary analysis by sampling trees. *BMC Evolutionary Biology*, **7**, 214.

Eck, S. (1984). Katalog der ornithologischen Sammlung Dr. Udo Bährmanns (3. Fortsetzung). *Zoologische Abhandlungen, Museum für Tierkunde Dresden*, **39**, 71–98.

Eck, S. (1996). Die palaearktischen Vögel – Geospezies und Biospezies. *Zoologische Abhandlungen, Museum für Tierkunde Dresden*, **49**, Suppl., 1–103.

Eck, S., Fiebig, J., Fiedler, W., Heynen, I., Nicolai, B., Töpfer, T., van den Elzen, R., Winkler, R. & Woog, F. (2011). Measuring birds. Vögel vermessen. Wilhelmshaven, Deutsche Ornithologen-Gesellschaft.

Ericson, P. G. P., Klopfstein, S., Irestedt, M., Nguyen, J. M. T. & Nylander, J. A. A. (2014). Dating the diversification of the major lineages of Passeriformes (Aves). *BMC Evolutionary Biology*, **14**, 8.

Finlayson, C. (2011). *Avian Survivors: The History and Biogeography of Palearctic Birds*. London, T. & A. D. Poyser.

Forrest, M., Eronen, J. T., Utescher, T., Knorr, G., Stepanek, C., Lohmann, G. & Hickler, T. (2015). Climate-vegetation modelling and fossil plant data suggest low atmospheric CO2 in the late Miocene. *Climate of the Past*, **11**, 1701–1732.

Funk, D. J. & Omland, K. E. (2003). Species-level paraphyly and polyphyly: Frequency, causes and consequences with insights from animal mitochondrial DNA. *Annual Review of Ecology, Evolution and Systematics*, **34**, 397–423.

Fulton, T. L. (2012). Setting up an ancient DNA laboratory, pp. 1–11 *in*: Shapiro, B & Hofreiter, M. (eds) *Ancient DNA: Methods and Protocols*. *Methods in Molecular Biology*. Berlin, Springer.

Gill, F., Donsker, D. & Rasmussen, P. (eds) (2020). IOC World Bird List (v10.1). doi:10.14344/IOC.ML.10.1. (last accessed on 20 April 2020).

GLUTZ V. BLOTZHEIM, U. N. & BAUER, K. M. (eds) (1993). *Handbuch der Vögel Mitteleuropas, Band **13/I***. Wiesbaden, Aula Verlag.

GREENWAY, J. C. (1967). Family Sittidae, pp. 124–144 *in*: PAYNTER, R. A. & MAYR, E. (eds) *Checklist of the Birds of the World – A Continuation of the Work of James L. Peters. Volume **XII***. Cambridge, Massachusetts, Museum of Comparative Zoology.

GROTH, J. G. & BARROWCLOUGH, G. F. (1999). Basal divergences in birds and the phylogenetic utility of the nuclear RAG-1 gene. *Molecular Phylogenetics and Evolution*, **12,** 115–123.

GUO, Z., PENG, S., HAO, Q., BISCAYE, P. E., AN, Z. & LIU, T. (2004). Late Miocene-Pliocene development of Asian aridification as recorded in the Red-Earth formation in northern China. *Global and Planetary Change*, **41**, 135–145.

HAHN, C., BACHMANN, L. & CHEVREUX, B. (2013). Reconstructing mitochondrial genomes directly from genomic next-generation sequencing reads – a baiting and iterative mapping approach. *Nucleic Acids Research*, **41**, 1–9.

HARING, E., GAMAUF, A. & KRYUKOV, A. (2007). Phylogeographic patterns in widespread corvid birds. *Molecular Phylogenetics and Evolution*, **45**, 840–862.

HARING, E., DÄUBL, B., PINSKER, W., KRYUKOV., A. & GAMAUF, A. (2012). Genetic divergences and intraspecific variation in corvids of the genus *Corvus* (Aves: Passeriformes: Corvidae) – a first survey based on museum specimens. *Journal of Zoological Systematics and Evolutionary Research*, **50**, 230–246.

HARRAP, S. & QUINN, D. (eds) (1996). *Tits, Nuthatches & Treecreepers*. Princeton, N. J., Princeton University Press.

HARRAP, S. (2008). Family Sittidae (Nuthatches), pp. 102-145 *in*: DEL HOYO, J., ELLIOT A., CHRISTIE, D., ARLOTT, N., BURN, H. (eds) (2008). *Handbook of the Birds of the World. Vol **13**. From Penduline-tits to Shrikes*. Barcelona, Lynx Edicions.

HEBERT, P.D.N., STOECKLE, M.Y., ZEMLAK, T.S. & FRANCIS, C.M. (2004). Identification of birds through DNA barcodes. *PLOS Biology*, **2,** e312.

HELBIG, A. J., MARTENS, J., SEIBOLD, I., HENNIG, F., SCHOTTLER, B. & WINK, M. (1996). Phylogeny and species limits in the Palaearctic chiffchaff *Phylloscopus collybita* complex: Mitochondrial genetic differentiation and bioacoustic evidence. *Ibis*, **138**, 650–666.

HEWITT, G. M. (2000). The genetic legacy of the Quarternary Ice Ages. *Nature*, **405**, 907–913.

HEWITT, G. M. (2004). The structure of biodiversity–insights from molecular phylogeography. *Frontiers in Zoology*, **1**, 4.

HORN, S. (2012). Target enrichment via DNA hybridization capture, pp. 177–188 *in*: SHAPIRO, B & HOFREITER, M. (eds) *Ancient DNA: Methods and Protocols*. *Methods in Molecular Biology, **840***. Berlin, Springer.

HUNG, C., DROVETSKI, S. V. & ZINK, R. M. (2012). Multilocus coalescence analyses support a mtDNA-based phylogeographic history for a widespread Palearctic passerine bird, *Sitta europaea*. *Evolution*, **66**, 2850–2864.

ILLERA, J. C., RICHARDSON, D. S., HELM, B., ATIENZA, J. C. & EMERSON, B. C. (2008). Phylogenetic relationships, biogeography and speciation in the avian genus *Saxicola*. *Molecular Phylogenetics and Evolution*, **48**, 1145–1154.

INSKIPP, C. & INSKIPP, T. (eds) (1991). *A Guide to the Birds of Nepal. 2nd edition*. London, Christopher Helm.

JACQUES, F. M. B., SHI, G. & WANG, W. (2013). Neogene zonal vegetation of China and the evolution of the winter monsoon. *Bulletin of Geosciences*, **88**, 175–193.

JIANG, H., LEI, R., DING, S. W. & ZHU, S. (2014). SKEWER: a fast and accurate adapter trimmer for next-generation sequencing paired-end reads. *BMC Bioinformatics*, **15**, 182.

JOHANNSSON, U. S. & ERICSON, P. G. P. (2005). A re-evaluation of basal phylogenetic relationships within trogons (Aves: Trogonidae) based on nuclear DNA sequences. *Journal of Zoological Systematics and Evolutionary Research*, **43**, 166–173.

JOHANSSON, U. S., ALSTRÖM, P., OLSSON, U., ERICSON, P. G. P., SUNDBERG, P. & PRICE, T. D. (2007). Build-up of the Himalayan avifauna through immigration: a biogeographical analysis of the *Phylloscopus* and *Seicercus* warblers. *Evolution*, **61**, 324–333.

KINDLER, C. & FRITZ, U. (2018). Phylogeography and taxonomy of the barred grass snake (*Natrix helvetica*), with a discussion of the subspecies category in zoology. *Vertebrate Zoology*, **68**, 269–281.

KIZIRIAN, D. & DONNELLY, M. A. (2004). The criterion of reciprocal monophyly and classification of nested diversity at the species level. *Molecular Phylogenetics and Evolution*, **32**, 1072–1076.

KRAJEWSKI, C., SIPIORSKI, J. T. & ANDERSON, F. E. (2010). Complete mitochondrial genome sequences and the phylogeny of cranes (Gruiformes: Gruidae). *The Auk*, **127**, 440–452.

KRYUKOV, A., IWASA, M. A., KAKIZAWA, R., SUZUKI, H., PINSKER, W. & HARING, E. (2004). Synchronic east-west divergence in azure-winged magpies (*Cyanopica cyanus*) and magpies (*Pica pica*). *Journal of Zoological Systematics and Evolutionary Research*, **42**, 342–351.

KRYUKOV, A. P., SPIRIDONOVA, L. N., MORI, S., ARKHIPOV, V. Y., RED'KIN, Y. A., GOROSHKO, O. A., LOBKOV, E. G. & HARING, E. (2017). Deep phylogeographic breaks in magpie *Pica pica* across the Holarctic: concordance with bioacoustics and phenotypes. *Zoological Science*, **34**, 185–200.

KUMAR, S., STECHER, G. & TAMURA, K. (2016). MEGA7: Molecular Evolutionary Genetics Analysis version 7.0 for bigger datasets. *Molecular Biology and Evolution*, **33**, 1870–1874.

KVIST, L., MARTENS, J., HIGUCHI, H., NAZARENKO, A. A., VALCHUK, O. P. & ORELL, M. (2003). Evolution and genetic structure of the great tit (*Parus major*) complex. *Proceedings of the Royal Society B: Biological Sciences*, **270**, 1447–1454.

LANFEAR, R., CALCOTT, B., HO, S. Y. W. & GUINDON, S. (2012). PartitionFinder: combined selection of partitioning schemes and substitution models for phylogenetic analyses. *Molecular Biology and Evolution*, **29**, 1695–1701.

LEONOVICH, V. V., DEMINA, G. V. & VEPRINTSEVA, O. D. (1996). [*Sitta europaea* L. & "small" nuthatches *S. villosa* VERREAUX and *S. krueperi* PELZELN: problems of taxonomy and phylogeny.]. *Bjulleten' Moskovskogo Obscestva Ispytatelej Prirody / Otdel biologiceskij*, **101**, 37–49. [In Russian, English summary].

LERNER, H. R. L., MEYER, M., JAMES, H. F., HOFREITER, M. & FLEISCHER, R. C. (2011). Multilocus resolution of phylogeny and timescale in the extant adaptive radiation of Hawaiian honeycreepers. *Current Biology*, **21**, 1–7.

MANEGOLD, A. (2008). Earliest fossil record of the Certhioidea (treecreepers and allies) from the early Miocene of Germany. *Journal of Ornithology*, **149**, 223–228.

MANISH, K. & PANDIT, M. K. (2018). Geophysical upheavals and evolutionary diversification of plant species in the Himalaya. *PeerJ*, **6**, e5919.

MARCHESE, C. (2015). Biodiversity hotspots: A shortcut for a more complicated concept. *Global Ecology and Conservation*, **3**, 297–309.

MARICIC, T., WHITTEN, M. & PÄÄBO, S. (2010). Multiplexed DNA sequence capture of mitochondrial genomes using PCR products. *PLoS ONE*, **5**, e14004.

MARTENS, J. & ECK, S. (1995). Towards an ornithology of the Himalayas. Systematics, ecology and vocalizations of Nepal birds. *Bonner Zoologische Monographien*, **38**, 1–445.

MARTENS, J., TIETZE, D. T. & PÄCKERT, M. (2011). Phylogeny, biodiversity, and species limits of passerine birds in the Sino-Himalayan region – A critical review. *Ornithological Monographs*, **70**, 64–94.

MARTIEN, K. K., LESLIE, M. S., TAYLOR, B. L., MORIN, P. A., ARCHER, F. I., HANCOCK-HANSER, B. L., ROSEL, P. E., VOLLMER, N. L., VIRICEL, A. & CIPRIANO, F. (2017). Analytical approaches to subspecies delimitation with genetic data. Analytical approaches to subspecies delimitation with genetic data. *Marine Mammal Science*, **33**, 27–55.

MATTHYSEN, E. (2010). *The Nuthatches*. San Diego, Academic Press.

MAYR, E. (1982). Of what use are subspecies? *Auk* **99**, 593–595.

MAYR, E. (1943). Criteria of subspecies, species and genera in ornithology. *Annals of the New York Academy of Sciences*, **44**, 133–139.

MEYER, M. & KIRCHER, M. (2010). Illumina sequencing library preparation for highly multiplexed target capture and sequencing. *Cold Spring Harbor Protocols*, doi:10.1101/pdb.prot5448.

Milne, I., Stephen, G., Bayer, M., Cock, P. J. A., Pritchard, L., Cardle, L., Shaw, P. D. & Marshall, D. (2013). Using tablet for visual exploration of second-generation sequencing data. *Briefings in Bioinformatics*, **14**, 193–202.

Moyle, R. G., Oliveros, C. H., Andersen, M. J., Hosner, P. A., Benz, B. W., Manthey, J. D. & Faircloth, B. C. (2016). Tectonic collision and uplift of Wallacea triggered the global songbird radiation. *Nature Communications*, **7**, 12709.

Nazarizadeh, M., Kaboli, M., Rezaie, H. R., Harisini, J. I. & Pasquet, E. (2016). Phylogenetic relationships of Eurasian Nuthatches (*Sitta europaea* Linnaeus, 1758) from the Alborz and Zagros Mountains, Iran. *Zoology in the Middle East*, **62**, 217–226.

Nylander, J. A. A. (2004). mrmodeltest v2. Program distributed by the author. Evolutionary Biology Centre, Uppsala University.

Oliveros, C. H., Field, D. J., Ksepka, D. T., Barker, F. K., Aleixo, A., Andersen, M. J., Alström, P., Benz, B. W., Braun, E. L., Braun, M. J., Bravo, G. A., Brumfield, R. T., Chesser, R. T., Claramunt, S., Cracraft, J., Cuervo, A. M., Derryberry, E. P., Glenn, T. C., Harvey, M. G., Hosner, P. A., Joseph, L., Kimball, R., Mack, A. L., Miskelly, C. M., Peterson, A. T., Robbins, M. B., Sheldon, F. H., Silveira, L. F., Smith, B. T., White, N. D., Moyle, R. G. & Faircloth, B. C. (2019). Earth history and the passerine superradiation. *Proceedings of the National Academy of Sciences*, **116**, 7916–792.

Opgenoorth, L., Vendramin, G. G., Mao, K., Miehe, G., Miehe, S., Liepelt, S., Liu, J. & Ziegenhagen, B. (2009). Tree endurance on the Tibetan Plateau marks the world's highest known tree line of the Last Glacial Maximum. *New Phytologist*, **185**, 332–342.

Päckert, M., Martens, J., Eck, S., Nazarenko, A. A., Valchuk, O. P., Petri, B. & Veith, M. (2005). *Parus major* – a misclassified ring species. *Biological Journal of the Linnean Society*, **86**, 153–174.

Päckert, M., Martens, J. & Sun, Y.H. (2010). Phylogeny of long-tailed tits and allies inferred from mitochondrial and nuclear markers (Aves: Passeriformes, Aegithalidae). *Molecular Phylogenetics and Evolution*, **55**, 952–967.

Päckert, M., Martens, J., Sun, Y.-H., Severinghaus, L. L., Nazarenko, A. A., Ting, J., Töpfer, T. & Tietze, D. T. (2012). Horizontal and elevational phylogeographic patterns of Himalayan and Southeast Asian forest passerines (Aves: Passeriformes). *Journal of Biogeography*, **39**, 556–573.

Päckert, M., Sun, Y.-H., Strutzenberger, P., Valchuk, O., Tietze, D. T. & Martens, J. (2015). Phylogenetic relationships of endemic bunting species (Aves, Passeriformes, Emberizidae, *Emberiza koslowi*) from the eastern Qinghai-Tibet Plateau. *Vertebrate Zoology*, **65**, 135–150.

Päckert, M., Sun, Y.-H. & Martens, J. (2018). Cradles of evolution – Hugo Weigold's biogeography of Tibet and the Sino-Himalayas in the light of molecular systematics and phylogeography, pp. 153-162 *in*: Hartmann, M., Barclay, M. & Weipert, J. (eds) *Biodiversity and Natural Heritage of the Himalaya VI*. Erfurt, Verein der Freunde und Förderer des Naturkundemuseums Erfurt e.V..

Paudayal, K. N. & Ferguson, D. K. (2004). Pleistocene palynology of Nepal. *Quarternary International*, **117**, 69–79.

Pasquet, E. (1998). Phylogeny of the nuthatches of the *Sitta canadensis* group and its evolutionary and biogeographic implications. *Ibis*, **140**, 150–156.

Pasquet, E., Barker, F. K., Martens, J., Tillier, A., Cruaud, C. & Cibois, A. (2014). Evolution within the nuthatches (Sittidae: Aves, Passeriformes): molecular phylogeny, biogeography, and ecological perspectives. *Journal of Ornithology*, **155**, 755–765.

Patten, M. A. (2015). Subspecies and the philosophy of science. *The Auk*, **132**, 481–485.

Patten, M. A., Winker, K. & Haig, S. (2010). Null expectations in subspecies diagnosis. *Ornithological Monographs*, **67**, 35.

Pentzold, S., Tritsch, C., Martens, J., Tietze, D. T., Giacalone, G., LoValvo, M., Nazarenko, A. A., Kvist, L. & Päckert, M. (2013). Where is the line? Phylogeography and secondary contact of western Palearctic coal tits (*Periparus ater*: Aves, Passeriformes, Paridae). *Zoologischer Anzeiger – A Journal of Comparative Zoology*, **252**, 360–367.

Philimore, A. B., & Owens, I. P. F. (2006). Are subspecies useful in evolutionary and conservation biology? *Proceedings of the Royal Society B*, **273**, 1049–1053.

Pons, J. M., Olioso, G., Cruaud, C. & Fuchs, J. (2011). Phylogeography of the Eurasian green woodpecker (*Picus viridis*). *Journal of Biogeography*, **38**, 311–325.

Pons, J. M., Masson, C., Olioso, & Fuchs, J. (2019). Gene flow and genetic admixture across a secondary contact zone between two divergent lineages of the Eurasian Green Woodpecker *Picus viridis*. *Journal of Ornithology*, **38**, 311–325.

Pound, M. J., Haywood, A. M., Salzmann, U. & Riding, J. B. (2012). Global vegetation dynamics and latitudinal temperature gradients during the Mid to Late Miocene (15.97–5.33 Ma). *Earth-Science Reviews*, **112**, 1–22.

Pratt, H. G. (2010). Revisiting species and subspecies of island birds for a better assessment of biodiversity. *Ornithological Monographs*, **67**, 79–89.

Price, T. D., Hooper, D. M., Buchanan, C. D., Johansson, U. S., Tietze, D. T., Alström, P., Olsson, U., Ghosh-Harihar, M., Ishtiaq, F., Gupta, S. K., Martens, J. Harr, B., Singh, P. & Mohan, D. (2014). Niche filling slows the diversification of Himalayan songbirds. *Nature*, **509**, 222–225.

R Core Team (2018). R: A language and environment for statistical computing. R Foundation for Statistical Computing, Vienna, Austria. URL https://www.R-project.org/.

Quillfeldt P. (2017). Body mass is less important than bird order in determining the molecular rate for bird mitochondrial DNA. *Molecular Ecology*, **26**, 2426–2429.

Rambaut, A. (2009). figtree version 1.2.2 – Computer program distributed by the author, website: http://tree.bio.ed.ac (last accessed on 29 November 2010).

Rambaut, A. & Drummond, A. J. (2007). tracer v1.4. http://beast.bio.ed.ac.uk/Tracer.

Ranhotra, P. S., Sharma, J., Battacharyya, A. & Basavaiah, N. (2017). Late Pleistocene – Holocene vegetation and climate from the paleaolake sediments, Rutki valley, Kinnaur, Himachal Himalaya. *Quarternary International*, **479**, 79–89.

Rasmussen, P. C. & Anderton, J. C. (2005). *Birds of South Asia: the Ripley Guide*. Barcelona, Lynx.

Red'kin, Y. A., Arkhipov, V. Y., Volkov, S. Y., Mosalov, A. A. & Koblik, E. A. (2016). Art oder keine Art? Strittige taxonomische Ansichten zu den Vögeln Nord-Eurasiens. *Ornithologische Mitteilungen*, **68**, 324–354.

Red'kin, Y. & Konovalova, M. (2006). Systematic notes on Asian birds. 63. The eastern Asiatic races of *Sitta europaea* Linneaus, 1758. *Zoologische Mededelingen*, **80**, 241–261.

Rising, J. D. (2007). Named subspecies and their significance in contemporary ornithology. *Ornithological Monographs*, **63**, 45–54

Sangster, G. (2014). The application of species criteria in avian taxonomy and its implications for the debate over species concepts. *Biological Reviews*, **89**, 199–214.

Sangster, G., Collinson, J. M., Crochet, P.-A., Knox, A. G., Parkin, D. T. & Votier, S. C. (2012). Taxonomic recommendations for British birds: eighth report. *Ibis*, **154**, 874–883.

Santos, A. M., Cabezas, M. P., Tavares, A. I., Xavier, R. & Branco, M. (2016). tcsBU: a tool to extend tcs network layout and visualization. *Bioinformatics*, **32**, 627–628 (doi: 10.1093/bioinformatics/btv636).

Schmitt, T.(2007).Molecular biogeography of Europe: Pleistocene cycles and postglacial trends. *Frontiers in Zoology*, **4**, 11.

Silvestro, D. & Michalak, I. (2012). raxmlgui: a graphical front-end for raxml. *Organisms Diversity and Evolution*, **12**, 335–337.

Song, G., Zhang, R., Qu, Y., Wang, Z., Dong, L., Kristin, A., Alström, P., Ericson, P. G. P., Lambert, D. M., Fjeldså, J & Lei, F. (2016). A zoogeographical boundary between the Palaearctic and Sino-Japanese realms documented by consistent north/south phylogeographical divergences in three woodland birds in eastern China. *Journal of Biogeography*, **43**, 2099–2112.

SONG, G., ZHANG, R., ALSTRÖM, P., IRESTEDT, M., CAI, T., QU, Y., ERICSON, P. G. P., FJELDSÅ, J. & LEI, F. (2018). Complete taxon sampling of the avian genus *Pica* (magpies) reveals ancient relictual populations and synchronous Late-Pleistocene demographic expansion across the Northern Hemisphere. *Journal of Avian Biology*, **49**, jav-01612.

SORENSON, M. D., AST, J. C., DIMCHEFF, D. E., YURI, T. & MINDELL, D. P. (1999). Primers for a PCR-Based Approach to Mitochondrial Genome Sequencing in Birds and Other Vertebrates. *Molecular Phylogenetics and Evolution*, **12**, 105–114.

SPELLMAN, G. M. & KLICKA, J. (2006). Testing hypotheses of Pleistocene population history using coalescent simulations: phylogeography of the pygmy nuthatch (*Sitta pygmaea*). *Proceedings of the Royal Society B, Biological Sciences*, **273**, 3057–3063.

SPELLMAN, G. M. & KLICKA, J. (2007). Phylogeography of the white-breasted nuthatch (*Sitta carolinensis*): diversification in North American pine and oak woodlands. *Molecular Ecology*, **16**, 1729–1740.

STAMATAKIS, A. (2006). RAXML-VI-HPC: maximum likelihood-based phylogenetic analyses with thousands of taxa and mixed models. *Bioinformatics*, **22**, 2688–2690.

STRESEMANN, E. (1919). *Sitta europaea homeyeri*: eine reine Rasse oder eine Mischrasse? *Verhandlungen der Ornithologischen Gesellschaft Bayern*, **14**, 139–147.

TAMURA, K., PETERSON, D., PETERSON, N., STECHER, G., NEI, M. & KUMAR, S. (2011). MEGA5: molecular evolutionary genetics analysis using maximum likelihood, evolutionary distance, and maximum parsimony methods. *Molecular Biology and Evolution*, **28**, 2731–2739.

TIETZE, D. T., MARTENS, J. & SUN, Y. H., SEVERINGHAUS, L. L. & PÄCKERT, M. (2011). Song evolution in the coal tit *Parus ater*. *Journal of Avian Biology*, **42**, 214–230.

TOTODU & SHYAMAL, L. (2008). Illustration of Nuthatches, Sittidae of the world. Downloaded from https://commons.wikimedia.org/wiki/File:Sittidae.svg, (last accessed on 17 November 2015).

TRITSCH, C., MARTENS, J., SUN Y.-H., HEIM, W., STRUTZENBERGER, P. & PÄCKERT, M. (2017). Improved sampling at the subspecies level solves a taxonomic dilemma – A case study of two enigmatic Chinese tit species. *Molecular Phylogenetics and Evolution*, **107**, 538–550.

TRITSCH, C., STUCKAS, H., MARTENS, J., PENTZOLD, S., KVIST, L., LO VALVO, M., GIACALONE, G., TIETZE, D. T., NAZARENKO, A. A. & PÄCKERT, M. (2018). Gene flow in the European coal tit, *Periparus ater* (Aves: Passeriformes): low among Mediterranean populations but high in a continental contact zone. *Biological Journal of the Linnean Society*, **124**, 319–338.

VAURIE, C. (1950). Notes on some Asiatic nuthatches and creepers. *American Museum Novitates*, **1472**, 1–39.

VAURIE, C. (1959). *The birds of the Palearctic Fauna. A Systematic Reference. Order Passeriformes*. London, Witherby.

VOELKER, G. (2010). Repeated vicariance of Eurasian songbird lineages since the Late Miocene. *Journal of Biogeography*, **37**, 1251–1261.

VOOUS, K. H. & VAN MARLE, J. G. (1953). The distributional history of the Nuthatch, *Sitta europaea* L. *Ardea*, **41** (suppl.), 1–68.

WALLIN, H., KVAMME, T. & BERGSTEN, J. (2017). To be or not to be a subspecies: description of *Saperda populnea lapponica* ssp. n. (Coleoptera, Cerambycidae) developing in downy willow (*Salix lapponum* L.). *ZooKeys*, **691**, 103–148.

WALSTROM, V. W., KLICKA, J. & SPELLMAN, G. M. (2011). Speciation in the White-breasted Nuthatch (*Sitta carolinensis*): a multilocus perspective. *Molecular Ecology*, **21**, 907–20.

WANG, W., DAI, C., ALSTRÖM, P., ZHANG, C., QU, Y., LI, S.-H., YANG, X., ZHAO, N., SONG, G. & LEI, F. (2014). Past hybridization between two East Asian long-tailed tits (*Aegithalos bonvaloti* and *A. fuliginosus*). *Frontiers in Zoology*, **11**, 40.

WANG, H., LU, H., ZHAO, L., ZHANG, H., LEI, F. & WANG, Y. (2019). Asian monsoon rainfall variation during the Pliocene forced by global temperature changes. *Nature Communications*, **10**, 5272.

WEIGOLD, H. (2005). *Die Biogeographie Tibets und seiner Vorländer*. Halle/Saale, Verein Sächsischer Ornithologen e.V.

WEIR, J. T. & SCHLUTER, D. (2007). The latitudinal gradient in recent speciation and extinction rates in birds and mammals. *Science*, **315**, 1574–1576.

WEIR, J. T. & SCHLUTER, D. (2008). Calibrating the avian molecular clock. *Molecular Ecology*, **17**, 2321–2328.

WICKHAM, H. (2016). ggplot2: Elegant Graphics for Data Analysis. New York, Springer.

WIKRAMANAYAKE, E. D., DINERSTEIN, E. & LOUCKS, C. J. (2002). *Terrestrial Ecoregions of the Indo-Pacific: A Conservation Assessment*. Washington D.C., Island Press.

WILSON, E. O., & BROWN, W. L. (1953). The subspecies concept and its taxonomic application. *Systematic Zoology*, **2**, 97–111.

ZHANG, R., SONG, G., QUA, Y., ALSTRÖM, P., RAMOS, R., XING, X., ERICSON, P. G. P., FJELDSÅ, J., WANG, H., YANG, H., KRISTIN, A., SHESTOPALOVJ, A. M., CHOE, J. C. & LEI, F. (2012). Comparative phylogeography of two widespread magpies: Importance of habitat preference and breeding behavior on genetic structure in China. *Molecular Phylogenetics and Evolution*, **65**, 562–572.

ZHAO, M., ALSTRÖM, P., OLSSON, U., QU, Y. & LEI, F. (2016). Phylogenetic position of the Wallcreeper *Tichodroma muraria*. *Journal of Ornithology*, **157**, 913–918.

ZHAO, M., CHANG, Y., KIMBALL, R. T., ZHAO, J., LEI, F. & QU, Y. (2019). Pleistocene glaciation explains the disjunct distribution of the Chestnut-vented Nuthatch (Aves, Sittidae). *Zoologica Scripta*, **48**, 33–45.

ZINK, R. M. (2004). The role of subspecies in obscuring avian biological diversity and misleading conservation policy. *Proceedings of the Royal Society B*, **271**, 561–564.

ZINK, R. M., DROVETSKI S. V. & ROHWER, S. (2006). Selective neutrality of mitochondrial ND2 sequences, phylogeography and species limits in *Sitta europaea*. *Molecular Phylogenetics and Evolution*, **40**, 679–686.

ZINK, R. M., PAVLOVA, A., DROVETSKI, S., WINK, M. & ROHWER, S. (2009). Taxonomic status and evolutionary history of the *Saxicola torquata* complex. *Molecular Phylogenetics and Evolution*, **52**, 769–773.

Electronic Supplement Files

at http://www.senckenberg.de/vertebrate-zoology

VZ_70-2_Paeckert_Electronic_Supplements.zip

DOI: 10.26049/VZ70-2-2020-10/1

Fig. S1. Statistical parsimony network of COI sequence data (581 bp; $n = 42$).

Fig. S2. Variation of ventral plumage color in *Sitta europaea homeyeri*, from intensely buff-breasted (left) to nearly entirely white-breasted (right); specimens from the collection of the ZFMK, Bonn; areas: western Black Sea coast (Ropotamo, Bosna Strandzha, Bulgaria); southern Baltic Sea coast (Kaliningrad, Russia; Lusiny, Poland; Livland; Winckenburg).

Table S1. Origin of samples used for molecular analysis and multilocus tree reconstruction